Chapter 3
Quasi-Classical Theory of Bremsstrahlung on an Atom and an Ion with a Core

The quasi-classical theory of Bs on atoms and ions plays an important role in a number of applications such as radiation in partially ionized plasma, low-temperature plasma, gas discharge, absorption of radiation by plasma media, etc.

Stated in this chapter is the theory of spontaneous Bs, including the polarization channel, in scattering of electrons by atoms and ions with a core with fulfilment of the quasi-classical condition

$$\frac{Z e^2}{\hbar \mathrm{v}} \geq 1, \tag{3.1}$$

where Z is the charge number of an atom (ion), v is the electron velocity. In this chapter the Gaussian system of units is used.

As seen from the formula (3.1), a quasi-classical electron should be rather slow in contrast to a Born electron, for which the inequation (2.1) reverse of the relation (3.1) is true. It should be noted that the Born inequation is "strong", and the quasi-classical inequation is "weak".

The condition (3.1) is realized, for example, for low-temperature plasma. In this case by the charge number of an atomic (ion) nucleus and the electron velocity their average values defined by the state of a substance should be meant.

3.1 Classical Consideration in the Approximation of Straight Trajectories

3.1.1 Ordinary (Static) Bremsstrahlung

As is known, emission of a photon in scattering of a charged particle on an atom (ion, molecule, cluster, etc.) is called *bremsstrahlung*. The initial and final states of an emitting particle in this process belong to the continuous spectrum, and radiant

V. Astapenko, *Polarization Bremsstrahlung on Atoms, Plasmas, Nanostructures and Solids*, Springer Series on Atomic, Optical, and Plasma Physics 72,
DOI 10.1007/978-3-642-34082-6_3, © Springer-Verlag Berlin Heidelberg 2013

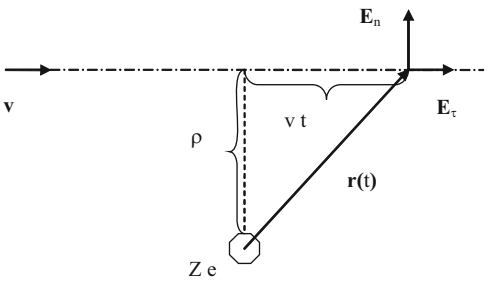

Fig. 3.1 The diagram of electron scattering by a nucleus in the approximation of straight trajectories, ρ is the impact parameter

energy is got from its kinetic energy. Let us consider at first the most simple case, when a nonrelativistic electron is scattered by a "bare" nucleus (that is, a nucleus without bound electrons) with the charge number Z. We use the classical expression for the power of dipole radiation Q in terms of the acceleration of a scattered electron $\mathbf{w}$ (the acceleration of a nucleus can be neglected due to its large mass) [1]:

$$Q(t) = \frac{2\,e^2}{3\,c^3}\,\mathbf{w}^2(t). \tag{3.2}$$

The total energy of bremsstrahlung for the whole time of collision is:

$$\Delta \mathrm{E} = \frac{4\,e^2}{3\,c^3}\int\limits_0^\infty |\mathbf{w}(\omega)|^2\,\frac{d\omega}{2\,\pi}. \tag{3.3}$$

In derivation of Eq. 3.3 the relation was used:

$$\int\limits_{-\infty}^{\infty} f^2(t)\,dt = 2\int\limits_0^\infty |f(\omega)|^2\,\frac{d\omega}{2\,\pi}, \tag{3.4}$$

where $f(t)$ is the real function of time, $f(\omega)$ is its Fourier component.

To calculate the Fourier component of the acceleration $\mathbf{w}(\omega)$, it is necessary to concretize the character of motion of a particle. It is well known that in case of a central force field the moment of momentum of an electron is $M = m\,\mathrm{v}\,\rho$, where v is the electron velocity (infinitely far from the nucleus), ρ is the impact parameter (see Fig. 3.1).

Thus the motion of a particle in the potential $U(r = |\mathbf{r}|)$ is characterized by two values: the initial velocity and the impact parameter, so the Fourier component of acceleration depends also on ρ: $\mathbf{w}(\omega) \to \mathbf{w}_\rho(\omega)$. For the last value we have:

$$\mathbf{w}_\rho(\omega) = \frac{e}{m}\,\mathbf{E}(\omega, \rho), \tag{3.5}$$

where $\mathbf{E}(\omega, \rho)$ is the Fourier component of the intensity of the nuclear electric field acting on a scattered electron with a specified impact parameter.

Let us calculate $\mathbf{E}(\omega, \rho)$ in the approximation *of straight trajectories* of electron motion. This approximation is true for "distant" collisions, when $\rho > a_C$ ($a_C = Z\,e^2/m\,\mathrm{v}^2$ is the Coulomb length). It should be noted that this approach was used by E. Fermi in calculation of excitation of atoms by charged particles [2]. Using the elementary electrodynamic formulas, we find for the Fourier component of nuclear electric field intensity:

$$\mathbf{E}(\omega, \rho) = \frac{2\,Z\,e}{\rho\,\mathrm{v}} \left\{ F\left(\frac{\omega\,\rho}{\mathrm{v}}\right) \mathbf{e}_n - iF'\left(\frac{\omega\,\rho}{\mathrm{v}}\right) \mathbf{e}_\tau \right\}, \tag{3.6}$$

where $\mathbf{e}_{n,\,\tau}$ are the normal and tangent (with respect to the velocity vector $\mathbf{v}$) unit vectors (see Fig. 3.1);

$$F(\zeta) = \int_0^\infty \frac{\cos(\zeta\,x)}{(1+x^2)^{3/2}}\,dx, \tag{3.7}$$

the prime designates differentiation with respect to the argument.

From the formula (3.3) in view of Eq. 3.5 the following expression for bremsstrahlung energy differential with respect to the photon frequency:

$$\frac{d\mathrm{E}_\rho}{d\omega} = \frac{2\;e^4}{3\,\pi\,m^2\,c^3}\,|\mathbf{E}(\omega, \rho)|^2. \tag{3.8}$$

The probability of bremsstrahlung in scattering of an electron with a specified impact parameter and frequency is related to the energy of Eq. 3.8 by the relation:

$$\frac{dW_\rho}{d\omega} = \frac{1}{\hbar\,\omega}\,\frac{d\mathrm{E}_\rho}{d\omega}, \tag{3.9}$$

and spectral cross-section of the process is:

$$\frac{d\sigma}{d\omega} = 2\,\pi \int_{\rho\,\mathrm{min}}^{\rho\,\mathrm{max}} \frac{dW_\rho}{d\omega}\,\rho\,d\rho, \tag{3.10}$$

where ρ_{min}, ρ_{max} are the minimum and maximum impact parameters. Assembling the formulas (3.8), (3.9) and (3.10), we obtain:

$$\frac{d\sigma}{d\omega} = \frac{4\;e^4}{3\;m^2\,c^3\,\hbar\,\omega} \int_{\rho\,\mathrm{min}}^{\rho\,\mathrm{max}} |\mathbf{E}(\omega, \rho)|^2\,\rho\,d\rho. \tag{3.11}$$

Hence in the approximation of straight trajectories we have for the spectral cross-section of bremsstrahlung of an electron on a "bare" nucleus:

$$\frac{d\sigma}{d\omega} = \frac{16\,Z^2\ e^6}{3\ m^2\,\mathrm{v}^2\,c^3\,\hbar\,\omega} \int\limits_{\rho\,\min}^{\rho\,\max} \frac{d\rho}{\rho} \left\{ F^2\left(\frac{\omega\,\rho}{\mathrm{v}}\right) + F'^2\left(\frac{\omega\,\rho}{\mathrm{v}}\right) \right\}, \tag{3.12}$$

where the function $F(\zeta)$ is given by the formula (3.7).

The classical consideration is found to be not sufficient to determine the limits of integration in Eq. 3.12 with respect to the impact parameter. For this purpose it is necessary to involve quantum considerations. Thus the minimum value $\rho_{\min}$ is defined by the de Broglie wavelength of a scattered electron:

$$\rho_{\min} \approx \lambda\!\!\!^{-}_{DB} = \frac{\hbar}{m\,\mathrm{v}}. \tag{3.13}$$

The relation (3.13) reflects the fact that the location of a quantum particle can not be determined more precisely than the spatial "diffusiveness" of its wave function that is characterized by the de Broglie wavelength. To determine the maximum impact parameter $\rho_{\max}$, it is necessary to use the energy conservation law in bremsstrahlung and the connection of change of a momentum of an incident electron with the value ρ: $\Delta p \approx \hbar/\rho$, then it is possible to obtain:

$$\rho_{\max} \approx \frac{\mathrm{v}}{\omega}. \tag{3.14}$$

In derivation of Eq. 3.14 the energy conservation law was used in the form $\hbar\,\omega = \mathbf{v}\ \boldsymbol{\Delta}\mathbf{p}$ true for small changes of the electron momentum $|\boldsymbol{\Delta}\mathbf{p}| \ll p$, which corresponds to the approximation of straight trajectories. This approximation realized in case of distant collisions $\rho > a_C$ implies the weakness of interaction of an incident particle with a target nucleus. It is natural that in weak interaction mainly low-frequency photons will be emitted. It can be shown that a corresponding condition looks like: $\omega < \omega_C$, where $\omega_C = \mathrm{v}/a_C$ is the Coulomb frequency. In the low-frequency region the argument of the function $F(\zeta)$ and of its derivative $F'(\zeta)$ is less than one: $\zeta = \omega\,\rho/\mathrm{v} < 1$, so, as it follows from the definition (3.7), it is possible to use the following approximate equations: $F(\zeta) \approx 1$ and $F'(\zeta) \approx 0$. As a result, instead of Eq. 3.12 we have:

$$\frac{d\sigma}{d\omega} = \frac{16\,Z^2\ e^6}{3\ m^2\,\mathrm{v}^2\,c^3\,\hbar\,\omega} \ln\left(\frac{\rho_{\max}}{\rho_{\min}}\right). \tag{3.15}$$

It is easy to generalize the obtained expression to an arbitrary scattered charged particle, for which the used approximations are fulfilled. For this purpose in the formulas (3.2) and (3.5) it is necessary to make replacements: $e \to e_p$, $m \to m_p$, where e_p, m_p are the charge and the mass of an incident particle. Then in view of

Eqs. 3.13 and 3.14 we come from Eq. 3.15 to the final expression for spectral bremsstrahlung of a nonrelativistic charged particle on a "bare" nucleus in the low-frequency approximation ($\hbar\,\omega << m_p\,\mathrm{v}^2/2$):

$$\frac{d\sigma}{d\omega} = \frac{16\,Z^2\;e^2\,e_p^4}{3\;m_p^2\,\mathrm{v}^2\,c^3\;\hbar\,\omega}\,\ln\left(\frac{m_p\,\mathrm{v}^2}{\hbar\,\omega}\right). \tag{3.16}$$

From the obtained equation it follows that the bremsstrahlung cross-section is *inversely proportional to the squared mass of an incident particle*. Thus, when going from light charged particles (electron, positron) to heavy particles (proton, alpha particle, etc.), the cross-section of the process under consideration decreases more than million times. This conclusion led to the well-known statement that heavy charged particles do not emit bremsstrahlung photons. As it will be clear from the following, this statement needs considerable correction.

The spectral intensity of emission is equal to the process cross-section multiplied by the incident particle flux and the energy of an emitted photon, so Eq. 3.16 gives:

$$\frac{dI}{d\omega} = \frac{16\,Z^2\;e^2\,e_p^4}{3\;m_p^2\,\mathrm{v}\,c^3}\,\ln\left(\frac{m_p\,\mathrm{v}^2}{\hbar\,\omega}\right). \tag{3.17}$$

As was already said, the formulas (3.16) and (3.17) were obtained in the approximation of distant collisions corresponding to emission of low-frequency photons. The contribution to bremsstrahlung of high-frequency photons $\omega > \omega_C$ is made by close collisions $\rho < a_C$ corresponding to *strongly curved trajectories*. The spectral cross-section and the intensity of bremsstrahlung of an electron in this case are described by the Kramers formulas:

$$\frac{d\sigma^{(Kram)}}{d\omega} = \frac{16\,\pi\,Z^2\;e^6}{3\,\sqrt{3}\;m^2\,\mathrm{v}^2\,c^3\;\hbar\,\omega}, \tag{3.18}$$

$$\frac{dI^{(Kram)}}{d\omega} = \frac{16\,\pi\,Z^2\;e^6}{3\,\sqrt{3}\;m^2\,\mathrm{v}\,c^3}. \tag{3.19}$$

The right side of the Eq. 3.19 does not include the Planck constant, which is indicative of the purely classical nature of this expression.

The formulas for bremsstrahlung of an electron scattered by the Coulomb center *beyond the approximation of straight trajectories* can be obtained by corresponding replacement of the Fourier transform of the electric field intensity $\mathbf{E}(\omega, \rho)$ by the function corresponding to motion in the Coulomb potential. This problem for a case of static Bs is considered in detail in the review [3] within the framework of so-called Kramers electrodynamics for motion of electrons along strongly curved trajectories.

It is interesting to note that the Kramers formulas (3.18) and (3.19) describe not only bremsstrahlung, but also photorecombination, when the final state of an emitting electron belongs to the discrete ion spectrum, that is, is bound. The said circumstance is a consequence of the fact that emission in the high-frequency limit $\omega > \omega_C$ is "gathered" from a section of the trajectory of the most approach to a nucleus, so an emitting electron "does not know" where it gets after emission of a photon.

The expressions (3.16) and (3.17) are obtained within the framework of the classical consideration with quantum "insertions" (3.13) and (3.14). It is clear that such an approach is not consistent, but its important advantage is physical transparency and mathematical simplicity. It is pertinent to note here that the use of the quantum-mechanical formalism within the framework of the *Born approximation* results in the same formulas for the cross-section and intensity of bremsstrahlung of low-frequency photons as Eqs. 3.16 and 3.17.

The criterion of the Born approximation (in the Gaussian system of units) is given by the inequation:

$$\frac{Z\left|e\,e_p\right|}{\hbar\,\mathrm{v}} << 1, \tag{3.20}$$

that is, corresponds to fast enough incident particles. The condition (3.20) allows calculation of the scattering cross-section by the perturbation theory with the ratio $Z\left|e\,e_p\right|/\hbar\,\mathrm{v}$ serving as a small parameter of the theory. The possibility of classical consideration is given by the inequation reverse of (3.20), so the above agreement of results is connected with the use of the approximation of straight trajectories, when the influence of a target on an electron is low as in the case of the Born approximation.

When going to bremsstrahlung on an atom, it is necessary to take into account the screening effect of bound electrons, which results in the replacement

$$\rho_{\max} \to \min(\mathrm{v}/\omega,\ r_a), \tag{3.21}$$

(r_a is the atomic radius) in the expressions for the cross-section and intensity of the process. Really, for the impact parameters $\rho > r_a$ the atomic field is close to zero, so the acceleration of an incident particle is negligible, and together with it, according to Eq. 3.2, bremsstrahlung is also absent. It is clear that screening is essential for low enough frequencies $\omega < \mathrm{v}/r_a$, otherwise an incident particle should fly close enough to a nucleus to emit a photon of a specified frequency.

In case of bremsstrahlung on multielectron atoms, when the Thomas-Fermi model "works", the Thomas-Fermi radius can be used as an atomic radius: $r_a \approx r_{TF} = a_B\, b/\sqrt[3]{Z}$, where $a_B \approx 0.53$ Å is the Bohr radius, Z is the charge number of the atomic nucleus, $b \cong 0.8553$ is the constant.

The replacement of Eq. 3.21 corresponds to the *screening approximation* in the bremsstrahlung theory used by Bethe and Heitler [4] in generalization of formulas for the process cross-section to an atomic case.

Physically the screening approximation means the replacement of atomic electrons by the distribution of electrostatic charge screening a nucleus. Thus bound electrons are excluded from consideration as a dynamic degree of freedom that can be excited during bremsstrahlung and can reradiate the electromagnetic field of an incident particle. Actually in emission of high-energy photons the energy-momentum excess can be transferred to atomic electrons, resulting in their excitation and ionization.

3.1.2 Polarization Bremsstrahlung

Besides the above real excitation, atomic electrons in case of collision of an atom with a charged particle can be excited *virtually*. Virtual excitation corresponds to appearance of a variable dipole moment in the atom that, according to the fundamentals of electrodynamics, should radiate electromagnetic waves. Such a process is called *polarization bremsstrahlung* since it is connected with the dynamic polarizability of an atom. The dynamic polarizability of an atom is considered in detail in Appendix 1. The dynamic polarizability of an atom together with the external variable field defines a radiating dipole moment.

Another interpretation can be given to polarization bremsstrahlung as a process of scattering of the eigenfield of an incident particle (a virtual photon) to the radiation field (a real photon) by atomic electrons. Polarization bremsstrahlung is an additional channel of radiation in charge scattering by a target having a system of bound electrons. We will call ordinary bremsstrahlung existing also on a "bare" nucleus ordinary or static bremsstrahlung. The last term implies that this channel is a single channel in the model of static distribution of electron charge of bound electrons.

Let us derive the formulas for polarization bremsstrahlung of a fast charged particle on an atom, considering the atom to be an elementary dipole with the polarizability $\alpha(\omega)$ (see Appendix 1, the formula (A.3) for connection of an induced dipole moment and the electric field strength).

For description of motion of an incident particle we use, as above, the classical approach and the approximation of straight trajectories. Again we proceed from the formula for the power of dipole radiation, but this time we will write it in terms of the dipole moment of the radiating system:

$$Q(t) = \frac{2}{3\,c^3}\left|\ddot{\mathbf{d}}(t)\right|^2. \tag{3.22}$$

Here two dots designate the second time derivative. Integrating the Eq. 3.22 with respect to time and using the formula (3.37) for the squared second derivative of the dipole moment, we come to the expression for the total energy of polarization bremsstrahlung for the whole time of collision corresponding to the impact parameter ρ:

$$\Delta \mathrm{E} = \frac{4\,e^2}{3\,c^3} \int\limits_0^\infty \omega^4 \left|\alpha(\omega)\,\mathbf{E}^{(p)}(\omega,\,\rho)\right|^2 \frac{d\omega}{2\,\pi}, \tag{3.23}$$

where $\mathbf{E}^{(p)}(\omega, \rho)$ is the Fourier component of the intensity of the electric field of an incident charged particle at the location of the atom. In derivation of this formula the relation was used: $\ddot{\mathbf{d}}(\omega) = -\omega^2\,\mathbf{d}(\omega)$ that follows from determination of the Fourier components.

Going from the total radiated energy to the spectral cross-section, as it was done in derivation of the formula (3.11), we obtain for polarization bremsstrahlung the following expression:

$$\frac{d\sigma^{PB}}{d\omega} = \frac{4\,\omega^3\,|\alpha(\omega)|^2}{3\;c^3\;\hbar} \int\limits_{\tilde{\rho}\,\mathrm{min}}^{\tilde{\rho}\,\mathrm{max}} \left|\mathbf{E}^{(p)}(\omega,\rho)\right|^2 \rho\,d\rho. \tag{3.24}$$

The upper limit of integration in this formula following from the energy conservation law is determined by the Eq. 3.14, the same as for static bremsstrahlung. The lower limit of integration is much different. In the elementary dipole approximation under consideration it is defined by the size of an atom:

$$\tilde{\rho}_{\mathrm{min}} = r_a. \tag{3.25}$$

As the analysis shows, scattering at low impact parameters $\rho < r_a$ makes a small contribution to the polarization bremsstrahlung cross-section since then coherence in reradiation of the eigenfield of an incident particle by atomic electrons to a real photon is lost.

From Fig. 3.1 it is easy to see that the Fourier component of the intensity of the electric field of an incident particle in the approximation of straight trajectories can be calculated by the formula similar to Eq. 3.6 with replacement of the nuclear charge by the incident particle (projectile) charge. As a result, for the intensity $\mathbf{E}^{(p)}(\omega, \rho)$ we have:

$$\mathbf{E}^{(p)}(\omega,\rho) = \frac{2\,e_p}{\rho\,\mathrm{v}} \left\{-F\left(\frac{\omega\,\rho}{\mathrm{v}}\right)\mathbf{e}_n + i\,F'\left(\frac{\omega\,\rho}{\mathrm{v}}\right)\mathbf{e}_\tau\right\}, \tag{3.26}$$

where $\mathbf{e}_n, \mathbf{e}_\tau$ are the normal and tangent unit vectors, the function $F(\zeta)$ is given by the Eq. 3.7. Shown in Fig. 3.2 is the modulus of the normal and tangential components of the electric field Eq. 3.26 as well as the entire spectrum $H(\nu) = \sqrt{F^2(\nu) + F'^2(\nu)}$ as a function of the dimensionless frequency $\nu = \omega\,\rho/\mathrm{v}$.

From Fig. 3.2 it is seen that the main contribution to the spectral function $H(\nu)$ in the region of its high values is made by the normal component of the electric field of an electron, and the spectrum width is of the order of the ratio v/ρ.

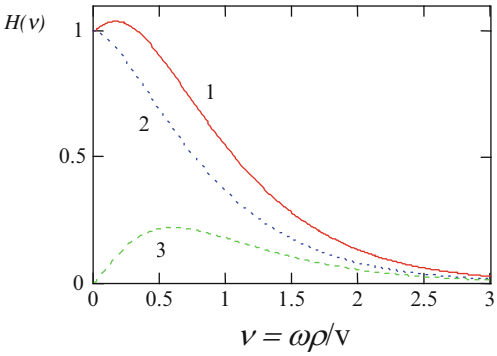

Fig. 3.2 The spectrum of the electric field of an incident particle (Eq. 3.26) as a function of the dimensionless frequency: *1* – entire spectrum, *2* – of the normal component of the field, *3* – of the tangent component of the field

Substituting Eq. 3.26 in Eq. 3.24, we obtain the spectral cross-section of polarization bremsstrahlung in the used approximation:

$$\frac{d\sigma^{PB}}{d\omega} = \frac{16\, e_p^2\, \omega^3\, |\alpha(\omega)|^2}{3\, \mathrm{v}^2\, c^3\, \hbar} \int_{r_a}^{\mathrm{v}/\omega} \frac{d\rho}{\rho} \left\{ F^2\left(\frac{\omega\, \rho}{\mathrm{v}}\right) + F'^2\left(\frac{\omega\, \rho}{\mathrm{v}}\right) \right\}. \tag{3.27}$$

Hence for intensity we find:

$$\frac{dI^{PB}}{d\omega} = \frac{16\, e_p^2\, \omega^4\, |\alpha(\omega)|^2}{3\, \mathrm{v}\, c^3} \int_{r_a}^{\mathrm{v}/\omega} \frac{d\rho}{\rho} \left\{ F^2\left(\frac{\omega\, \rho}{\mathrm{v}}\right) + F'^2\left(\frac{\omega\, \rho}{\mathrm{v}}\right) \right\}. \tag{3.28}$$

It should be noted that the formula (3.28) does not contain the Planck constant, which is indicative of its classical nature.

In the limit of low frequencies, when $F(\zeta) \approx 1$ and $F'(\zeta) \approx 0$, the formula (3.27) gives:

$$\frac{d\sigma^{PB}}{d\omega} = \frac{16\, e_p^2\, \omega^3\, |\alpha(\omega)|^2}{3\, \mathrm{v}^2\, c^3\, \hbar} \ln\left(\frac{\mathrm{v}}{\omega\, r_a}\right). \tag{3.29}$$

This expression is true for the frequencies $\omega < \mathrm{v}/r_a$, otherwise it is necessary to use the formula (3.27). Calculation, however, shows that in the frequency range $\omega > \mathrm{v}/r_a$ polarization bremsstrahlung is low.

The cross-section of Eq. 3.29 can be obtained within the framework of the quantum approach in case of truth of the Born approximation Eq. 3.20, that is, for fast (but nonrelativistic) incident particles.

It must be emphasized that the polarization bremsstrahlung cross-sections (3.27), (3.29) do not depend on the mass of an incident particle in contrast to the static bremsstrahlung cross-section (3.17). Thus the statement long existing in

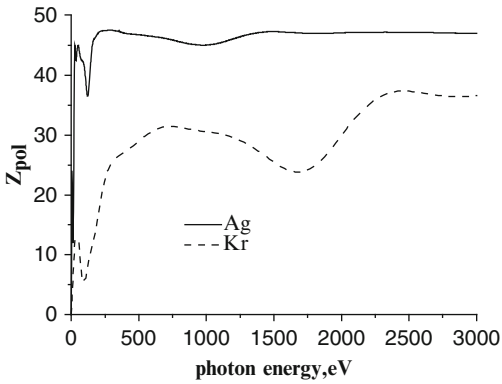

Fig. 3.3 The spectral dependence of the polarization charge of silver and krypton atoms

physics that heavy charged particles do not emit bremsstrahlung photons does not extend to the polarization channel. This circumstance is connected with the fact that the static bremsstrahlung cross-section is proportional to the squared acceleration of an incident particle, while the polarization channel cross-section the does not depend on this acceleration.

The polarization bremsstrahlung cross-section (3.29) can be obtained from the static process cross-section (3.16) with the use of replacements $m_p \to m, e_p^4 \to e^2\, e_p^2$, $\rho_{\min} \to \tilde{\rho}_{\min}$, and

$$Z \to Z_{pol}(\omega), \tag{3.30}$$

where

$$Z_{pol}(\omega) = \frac{m\,\omega^2}{e^2}\,|\alpha(\omega)| \tag{3.31}$$

is the effective polarization atomic charge (in the units of the electron charge e).

The polarization charge characterizes the ability of the electron core of an atom to emit a photon under the action of an ac field. In contrast to an ordinary charge, the polarization charge depends on the radiation frequency. The frequency dependence of the polarization charges of silver and krypton atoms is presented in Fig. 3.3.

From this figure it is seen that in the high-frequency range the polarization charge is equal to the number of bound electrons of an atom (or the charge number of its nucleus). This circumstance follows from the definition (3.31) and the formula for high-frequency polarizability (A.16). In the region of low frequencies $\omega \to 0$ the polarization charge according to Eq. 3.31 decreases quadratically since then the atomic polarizability is equal to its static value (A.15), that is, does not depend on frequency. Finally, in the intermediate spectral range the polarization charge is a nonmonotonic function that reflects the features of the energy spectrum of an atom. For example, a wide "dip" on the dashed curve of Fig. 3.3 in a range

of 1,600–1,750 eV corresponds to the energy of binding of $2p$ -electrons in a krypton atom. The minimum in the region of low frequencies corresponds to virtual excitation of subshells of an atom with the principal quantum number $n = 3$. Thus the spectral cross-section of polarization bremsstrahlung reflects the dynamics of the atomic core as a function of frequency.

In the high-frequency limit, when $\omega >> \omega_a$ (ω_a is the characteristic frequency of excitation of an atom in the discrete spectrum), but still $\omega < \mathrm{v}/r_a$, $\alpha(\omega) \approx -Z\,e^2/m\,\omega^2$ ($Z_{pol}(\omega) = Z$), and the formula (3.29) gives:

$$\frac{d\sigma^{PB}}{d\omega} = \frac{16\,Z^2\,e^4\,e_p^2}{3\,m^2\mathrm{v}^2\,c^3\hbar\,\omega}\,\ln\left(\frac{\mathrm{v}}{\omega\,r_a}\right). \tag{3.32}$$

Curiously, in case of an incident electron (positron) the obtained expression differs from the formula for the static bremsstrahlung cross-section (3.17) only by a logarithmic factor.

Now we will consider a resonant case, when the bremsstrahlung frequency is close to one of eigenfrequencies of an atom $\omega \approx \omega_0$, and dynamic polarizability looks like:

$$\alpha(\omega \approx \omega_0) \cong \frac{e^2}{m}\,\frac{f_0}{\omega_0^2 - \omega^2 - 2\,i\,\omega\,\delta_0}. \tag{3.33}$$

This expression for resonant polarizability follows from the general formula (A.14), if in it one resonant summand is retained, in which $\omega_{nm} \equiv \omega_0, f_{nm} \equiv f_0$ and $\delta_{nm} \equiv \gamma_0$. Substituting the formula (3.31) in Eq. 3.29, we obtain:

$$\frac{d\sigma^{res}}{d\omega} = \frac{4}{3}\,\frac{e_p^2}{\hbar\,c}\,\left(\frac{c}{\mathrm{v}}\right)^2\,\frac{r_e^2 f_0^2\,\omega_0}{(\omega_0 - \omega)^2 + \delta_0^2}\,\ln\left(\frac{\mathrm{v}}{\omega\,r_a}\right), \tag{3.34}$$

where $r_e = e^2/m\,c^2 \approx 2.8 \cdot 10^{-13}$ cm is the electron classical radius.

From the expression (3.34) it is seen that resonance polarization bremsstrahlung has a sharp maximum at the frequency $\omega = \omega_0$ if $\delta_0 << \omega_0$. The last inequation is satisfied in case of excitation of electrons of the outer atomic shell in the discrete spectrum, so for a neutral atom the energies of resonant photons are about 10 eV and less. In case of multiply charged ions having a system of bound electrons (an electron core) these energies can be much higher and reach a value of the order of several keV. Then, however, the transition damping constant equal to the Einstein coefficient A_{mn} is also great, and therefore the resonance becomes not such sharp. At frequencies corresponding to virtual excitation of inner atomic shells the resonance structure in the spectral dependence of the dynamic polarizability $\alpha(\omega)$ disappears. Instead of it, on the spectral curves "dips" arise that correspond to the beginning of photoionization of the atomic subshell (see Fig. 3.3).

3.2 Bremsstrahlung of Quasi-Classical Electrons in the Local Plasma Approximation for the Electron Core of a Target

The local plasma model (the Brandt-Lundqvist approximation [5]) for the polarizability of a multielectron target was considered in Sect. 2.4 (Sect. 2.4.1). This model was proposed for description of multielectron atoms, in which the electron–electron interaction in a specified (wide enough) spectral range can play a role comparable to the electron-nucleus interaction.

The Brandt-Lundqvist approximation can be considered as an elementary classical analog of the quantum-mechanical random phase exchange approximation widely used for taking into account electron–electron correlations in atomic physics. The main idea of this method is that electron–electron correlation effects are expressed in terms of the dynamic polarizability of the atomic core.

Such calculations in respect to the problem of calculation of the cross-section of polarization bremsstrahlung on an atom in a wide frequency range were carried out in the work [6] for electrons of kilovolt energies scattered by a krypton atom. It should be noted that such calculations represent a rather intricate numerical problem since wave functions of atomic electrons already in the zeroth approximation are the solutions of the Hartree-Fock integro-differential equations.

The high reliability of results obtained within the framework of the random phase exchange approximation shows the reverse side of the medal in necessity to carry out laborious calculations for each specific target and in difficulty of obtaining qualitative regularities "working" in a wide enough range of variation of problem parameters.

The purpose of this chapter is to develop semiquantitative methods of calculation of polarization effects in radiative processes on multielectron targets and to carry out the analysis of qualitative regularities of the said processes on their basis.

The main advantage of the used approach consists in its calculating simplicity and physical obviousness. Making no pretence of the exact quantitative description of the phenomenon, the method used in this chapter can be considered as an additional (to consistent quantum-mechanical calculations) method of description of polarization-interference effects on multielectron systems.

3.2.1 Polarizability of an Atom in the Brandt-Lundqvist Model

The dipole polarizability of an atom (or other multielectron system) is given within the framework of the local plasma frequency model by the formula (2.73) that can be rewritten as

$$\alpha^{BL}(\omega) = \int_0^{R_0} \frac{\omega_p^2(r)\, r^2\, dr}{\omega_p^2(r) - \omega^2 - i\,\delta} = \int \beta^{BL}(r,\omega)\; d\mathbf{r}, \tag{3.35}$$

where $\omega_p(r) = \sqrt{4\pi e^2 n(r)/m}$ is the local plasma frequency depending on the local electron density of the electron core $n(r)$, r is the distance from a point under consideration to the atomic nucleus, R_0 is the atomic radius. Here and further the spherical symmetry of the system is assumed, so $n(\mathbf{r}) = n(r)$.

The Eq. 3.35 gives the expression for dynamic polarizability as the volume integral of some dimensionless function $\beta^{BL}(r, \omega)$:

$$\beta^{BL}(r, \omega) = \frac{\omega_p^2(r)/4\,\pi}{\omega_p^2(r) - \omega^2 - i\,\delta}$$

that is natural to be called the *spatial density of the dynamic polarizability* of a target in the Brandt-Lundqvist approximation. This value in the local approximation under consideration is a liaison between the induced atomic polarization at the specified frequency $\mathbf{P}(r, \omega)$ and the strength of the external electric field $\mathbf{E}(r, \omega)$ causing this polarization, the cause and effect being taken at one point of space (local approximation):

$$\mathbf{P}(r, \omega) = \beta(r, \omega)\,\mathbf{E}(r, \omega). \tag{3.36}$$

In writing Eq. 3.36 it is assumed that the target has a spherical symmetry.

It should be noted that the expression (3.35) can be rewritten as the frequency integral if the spectral density of the oscillator strength is duly introduced by the formula

$$\frac{df}{d\omega} = \frac{m\,\omega^2}{e^2} r_p^2(\omega) \frac{dr_p(\omega)}{d\omega}, \tag{3.37}$$

where the function $r_p(\omega)$ is determined by solution of the equation

$$\omega = \omega_p(r). \tag{3.38}$$

Thus the dynamic polarizability in the Brandt-Lundqvist model can be formally presented in the characteristic quantum-mechanical form. The remaining difference consists in the fact that the Eq. 3.35 does not describe the contribution of the discrete spectrum to the atomic polarizability, which is natural since the local plasma frequency approximation is an essentially classical approximation. It should be noted that the contribution of the discrete spectrum is most essential for alkali-like ions and is small for systems with filled electron shells.

As easily seen from the formula (3.35), the high-frequency dynamic polarizability in the Brandt-Lundqvist model has correct asymptotics agreeing with the result of the quantum-mechanical calculation:

$$\alpha^{hf}(\omega) = -\frac{e^2\,N_e}{m\,\omega^2}, \tag{3.39}$$

where N_e is the full number of target electrons (see Appendix 1, the formula (A.16))

Table 3.1 Static polarizabilities of atoms and ions with filled shells (a.u.)

Atom (ion)	ArI	KrI	XeI	KII	RbII	CsII	SrIII	BaIII
α_0^{exp}	11	17	27	7.5	12	16.3	6.6	11.4
α_0^{var}	19.3	26.8	30.9	9.1	14.3	17.8	8.7	11.4
α_0^{VSh}		21.1	25.5	6.6	11.9	15.3	7.5	9.7
α_0^{BL}	22	24	27	8.6	11.6	13.5	7	8.4

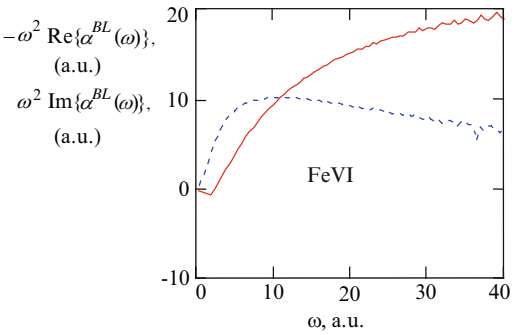

Fig. 3.4 The frequency dependences of the real (*solid line*) and imaginary (*dotted line*) parts of the dynamic polarizability of the iron ion calculated within the framework of the local plasma model

Given in Table 3.1 is the comparison of the values of static polarizabilities of atoms and ions (in atomic units) with filled electron shells calculated by different methods within the framework of the statistical description of an atom with experimental data (α_0^{exp}).

Here: α_0^{var} is the calculation by the variational method [7], α_0^{VSh} is the calculation of Vinogradov and Shevel'ko [8], $\alpha_0^{BL} = R_0^3/3$ is the calculation in the Brandt-Lundqvist model [5].

In calculations of static polarizability in the Brandt-Lundqvist model the radius of an atom (ion) was used that was calculated in view of the correlation allowance in the Thomas-Fermi-Dirac model.

From the given table it follows that in most cases for static polarizability the Brandt-Lundqvist method gives a satisfactory fit to the experiment for atoms (ions) with filled shells.

So from the analysis of low-frequency and high-frequency limits it can be expected that the use of the Brandt-Lundqvist model in the first approximation gives a reasonable approximation for the dynamic polarizability of an atom (ion).

Given in Fig. 3.4 are the frequency dependences of the values $\omega^2\,\mathrm{Re}\{\alpha(\omega)\}$ and $\omega^2\,\mathrm{Im}\{\alpha(\omega)\}$ for a FeVI ion calculated in the Brandt-Lundqvist approximation in a wide frequency range. The comparison with analogous dependences calculated in the random phase exchange approximation for a multielectron atom [6] shows that the calculation in the Brandt-Lundqvist model qualitatively correctly describes the

smoothed functions $\omega^2 \operatorname{Re}\{\alpha(\omega)\}$, $\omega^2 \operatorname{Im}\{\alpha(\omega)\}$ without considering peculiarities caused by the shell structure of an atom (maxima and minima near the thresholds of ionization of subshells).

Besides the Thomas-Fermi model for description of distribution of electron density of an atom, a number of improved models is used, such as the Thomas-Fermi-Dirac model and the Lenz-Jensen model [7]. Within the framework of these models the radius of a neutral atom R_0 is found to be a finite quantity in contrast to the Thomas-Fermi model, in which $R_0 \to \infty$. Moreover, for description of electron subshells the Slater wave functions are used that are distinguished by simplicity and ease in carrying out analytical calculations. These functions look like:

$$P_\gamma(r) = \sqrt{\frac{(2\beta)^{2\mu+1}}{\Gamma(2\mu+1)}} r^\mu e^{-\beta r}, \tag{3.40}$$

where $\gamma = (nl)$ is the set of quantum numbers characterizing an electronic state, β, μ are the Slater parameters that are chosen in a special manner to satisfy the experimental data on the energy of corresponding shells. The wave functions (3.40) are normalized, have correct asymptotics at long distances. With the use of the functions (3.40) the radial distribution of electron density of an atom in the Slater approximation can be obtained as

$$n(r) = \sum_\gamma N_\gamma P_\gamma^2(r). \tag{3.41}$$

The Slater electron density as well as the densities of other models of the atomic core can be used in calculation of the dynamic polarizability of an atom in the local plasma frequency approximation (3.35).

In more detail the methods of description of the core of multielectron atoms and ions, including statistical models, are stated in Appendix 2.

The results of calculation of the real and imaginary parts of the dipole dynamic polarizability of a krypton atom within the framework of the local plasma frequency method by the formula (3.35) with the use of electron density according to Slater and Lenz-Jensen are presented in Fig. 3.5. Shown in the same figure are the results of calculation of corresponding values in the quantum-mechanical random phase exchange approximation carried out in the work [6].

It is seen that the dynamic polarizability of a krypton atom calculated in the local plasma frequency model for Lenz-Jensen electron density in a smoothed manner renders the quantum-mechanical features of the frequency behavior of dynamic polarizability that are most pronounced near the potentials of ionization of electron subshells. Using the Slater wave functions within the framework of this model makes it possible to detect to some extent spectral fluctuations of polarizability near the potentials of ionization of electron subshells. In this case, however, the universality of description characteristic for the statistical model of an atom is violated.

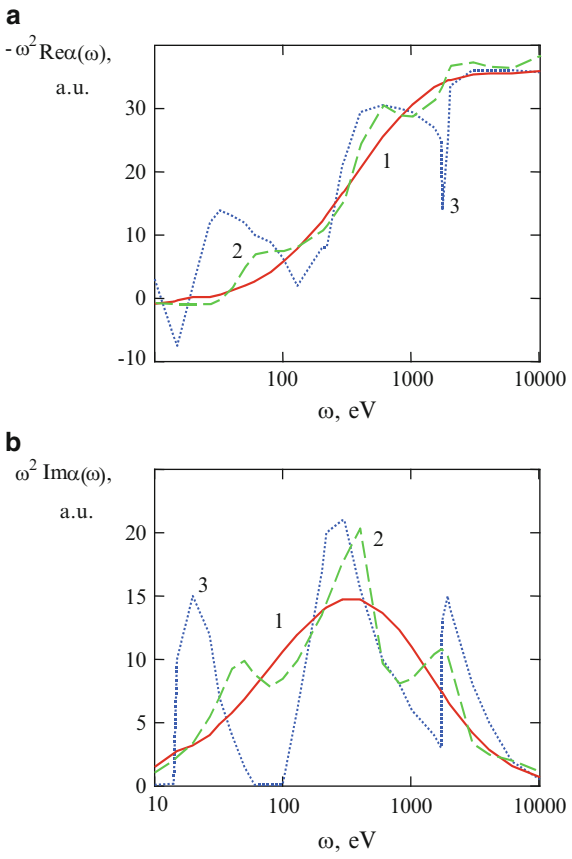

Fig. 3.5 The frequency dependences of the real (**a**) and imaginary (**b**) parts of the polarizability of a krypton atom calculated in different approximations: in the local plasma frequency approximation for Lenz-Jensen electron density (*1*), for Slater electron density (*2*), and in the random phase exchange approximation (*3*)

With the use of the formula (3.35) and the statistical model of an atom (see Appendix 2) for dynamic polarizability the following expression can be obtained:

$$\alpha(\omega, Z) = r_{TF}^3 \tilde{\alpha}\left(\frac{\omega}{Z}\right) = \frac{b^3 a_0^3}{Z} \tilde{\alpha}\left(\frac{\omega}{Z}\right), \tag{3.42}$$

$$\tilde{\alpha}(v) = \int_0^{x_0} \frac{4\pi f(x) x^2 \, dx}{4\pi f(x) - v^2 - i0}, \tag{3.43}$$

where $r_{TF} = b a_0 / Z^{1/3}$ is the Thomas-Fermi radius, Z is the charge of the atomic nucleus, a_0 is the Bohr radius, $b \cong 0.8853$, $\tilde{\alpha}(v)$ is the dimensionless polarizability as a function of the reduced frequency $v = \hbar\omega / 2Ry\, Z$, ($Ry = 13.6$ eV), $x_0 = R_0 / r_{TF}$ is the reduced atomic radius, $f(x)$ is the universal function describing the distribution of the electron density $n(r)$ in an atom within the framework of the statistical model according to the formula $n(r) = Z^2 f(r / r_{TF})$.

The explicit expressions for the function $f(x)$ for a number of statistical models, including the Thomas-Fermi and Lenz-Jensen models, are given in Appendix 2. For example, for the Lenz-Jensen function the formula (A.46) is true. Though the Thomas-Fermi function $\chi(x)$, in terms of which the concentration of atomic electrons (A.45) and the atomic potential are expressed, has no analytical representation, for this formula there are good approximations obtained by A. Sommerfeld. These approximations, both for neutral atoms and for multielectron ions, are also given in Appendix 2 (see the formulas (A.48), (A.49) (A.50)).

It must be emphasized that the dimensionless polarizability $\tilde{\alpha}(v)$ does not depend on the charge of an atomic nucleus. Thus the representation of the dynamic polarizability of a statistical atom (3.42) and (3.43) reveals the scaling law for this value with respect to the parameter v.

Let us give the high-frequency asymptotics of the dimensionless polarizability following from the formulas (3.42) and (3.43) with the help of the explicit form of the function $f(x)$ for the distribution of the Thomas-Fermi and Lenz-Jensen electron density (see Appendix 2). For the imaginary part of the dimensionless polarizability $\tilde{\alpha}(v)$ we have:

$$\mathrm{Im}\left\{\tilde{\alpha}^{T-F}(v \to \infty)\right\} \to \frac{4.35}{v^4}, \tag{3.44}$$

$$\mathrm{Im}\left\{\tilde{\alpha}^{L-J}(v \to \infty)\right\} \to \frac{4.615}{v^4}. \tag{3.45}$$

From the formulas (3.44) and (3.45) it is seen that the above statistical models give a close result for the imaginary part of polarizability. The high-frequency asymptotics of the real part of the dimensionless polarizability $\tilde{\alpha}(v)$ in both models of electron density of the atomic core look like

$$\mathrm{Re}\{\tilde{\alpha}(v \to \infty)\} \to -\frac{b^{-3}}{v^2}, \tag{3.46}$$

which is in the qualitative agreement with the general formula (3.39). From comparison of the expressions (3.44), (3.45) and (3.46) it follows in particular that at high frequencies the imaginary part of polarizability decreases much more rapidly than its real part.

Thus using the Brandt-Lundqvist model seems justified for the qualitative description of polarization effects on multielectron ions and atoms for frequencies $\omega \approx Z$ and more.

In the low-frequency range the use of the plasma-statistical approach can require some correction due to the fact that the potential of ionization of an atom within the framework of statistical models has an underestimated value, especially for targets with filled shells, so the characteristic features of the frequency dependence $\alpha(\omega)$ are found to be shifted to the region of low frequencies. So in calculation of cross-sections in the low-frequency range with the use of the Brandt-Lundqvist model for

the dynamic polarizability of a target it is worthwhile to shift the frequency dependence of polarizability to the region of high frequencies, so that the maximum of its imaginary part falls on the potential of ionization of an atom.

3.2.2 Polarization Potential in the Bremsstrahlung Theory

For calculation of the polarization bremsstrahlung cross-section we will introduce into consideration the potential of interaction of an incident particle with an ion being in the external uniform electromagnetic field $\mathbf{E}(\omega)$. This potential looks like

$$V_{pol}(\mathbf{R},\omega) = \int d\mathbf{r}\, \frac{\delta\rho(\mathbf{r},\omega)}{|\mathbf{r}-\mathbf{R}|}, \tag{3.47}$$

here $\delta\rho(\mathbf{r},\omega)$ is the spatial density of perturbation of an electron charge induced in the ion core under the action of the external field, $\mathbf{R}$ is the radius vector of an incident particle (IP).

It should be noted that the proposed approach is suited also for calculation of spontaneous processes: in this case by $\mathbf{E}(\omega)$ the field of quantum fluctuations should be understood.

The electron charge density perturbation $\delta\rho(\mathbf{r},\omega)$ is related with the polarization density induced in the ion core:

$$\delta\rho(\mathbf{r},\omega) = \text{div}\ \mathbf{P}(\mathbf{r},\omega). \tag{3.48}$$

The value $\mathbf{P}(\mathbf{r},\omega)$ in the *local approximation* is given by the formula (3.36).

The distribution of electron density in an atom (ion) everywhere in what follows we will assume to be spherically symmetric.

Assembling the written-out formulas and using the expansion of the reciprocal distance $|\mathbf{r}-\mathbf{R}|^{-1}$ in terms of spherical harmonics, after simple algebraic transformations and integration with respect to angular variables we obtain for the polarization potential in the local approximation the following expression:

$$V_{pol}(\mathbf{R},\omega) = e\frac{\mathbf{R}\mathbf{E}(\omega)}{R^3}\int_0^R \beta\,(r,\omega)\ 4\pi r^2 dr. \tag{3.49}$$

It is essential that this formula describes the *nondipole* potential of interaction of an IP with a perturbed ion core, which manifests itself in the presence of the magnitude of the IP radius vector in the upper limit of integration. This circumstance has a simple electrostatic interpretation: an external charge interacts only with part of the electron cloud inside the sphere of radius R.

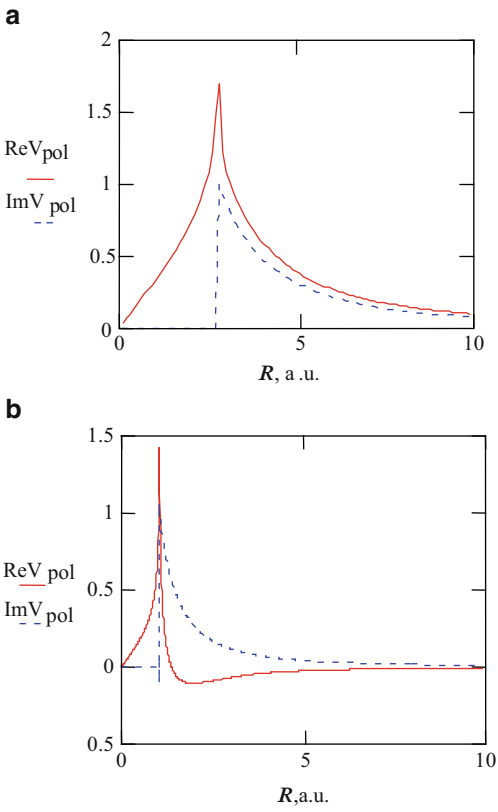

Fig. 3.6 The real and imaginary parts of the polarization potential normalized to the amplitude of the electromagnetic field at frequencies (**a**) $\omega = 0.9$ a.u., (**b**) $\omega = 3$ a.u. as functions of the distance to the nucleus of a *KII* ion. Calculation in the Brandt-Lundqvist approximation [5] with the use of the Thomas-Fermi-Dirac electron density

Thus the obtained polarization potential (Eq. 3.49) describes the effects connected with penetration of an IP into the ion core.

Presented in Fig. 3.6a, b are the results of calculation of the real and imaginary parts of the polarization potential normalized to the amplitude of the external electric field for a *KII* ion. The calculation was made in the local plasma approximation with the use of the electron density of the ion core in the Thomas-Fermi-Dirac model for two frequencies of the electromagnetic field $\omega = 0.9$ a.u. (a), 3 a.u. (b) by the formula (3.43). In both cases the real part of the polarization potential has a maximum at a distance determined by the Eq. 3.38. At this distance the local dielectric permittivity of a target becomes zero and at the same time an imaginary additive to the polarization potential appears. It is seen from the figure that the distance $r_p(\omega)$ (see Eq. 3.38) decreases with growing frequency. The function $r_p(\omega)$ in the Thomas-Fermi-Dirac model is monotonically decreasing since the spatial density of electron distribution in this model grows monotonically.

It is interesting to note that for any finite frequency $(0 < \omega < \infty)$ there is some distance to a nucleus $r_0(\omega)$ (and $r_0(\omega) > r_p(\omega)$), at which the real part of the polarization potential changes a sign. If it is taken into account that the interaction force is equal to the derivative of the potential taken with the minus sign, it can be

concluded from the form of the curves in Fig. 3.6 that at short enough distances from the nucleus an IP is effectively attracted to the target under the action of its polarization. At the same time at long distances the polarization interaction corresponds to repulsion.

Using the expression for the polarization potential (Eq. 3.49), it is possible to obtain the formula for a dipole moment induced in the ion core by a scattered particle if it is taken into account that:

$$V_{pol}(\mathbf{R},\,\omega) = -\mathbf{E}(\omega)\,\mathbf{D}_{pol}(\mathbf{R},\,\omega). \tag{3.50}$$

From comparison of Eqs. 3.49 and 3.50 we find

$$\mathbf{D}_{pol}(\mathbf{R},\omega) = -e_p\,\frac{\mathbf{R}}{R^3}\int\limits_0^R \beta\,(r,\omega)\,4\,\pi\,r^2\,dr. \tag{3.51}$$

The dipole moment $\mathbf{D}_{pol}(\mathbf{R},\omega)$ induced in the atomic core is a function of the external field frequency and the radius vector of an incident particle $\mathbf{R}$.

In view of the explicit expression for the spatial density of polarizability (3.35) from the formula (3.51) we find for the real and imaginary parts of the polarization dipole moment

$$\mathrm{Re}\left\{\mathbf{D}^{BL}(\omega,\,\mathbf{R})\right\} = e\,\frac{\mathbf{R}}{R^3}\,V.P.\int\limits_0^R \frac{\omega_p^2(r)\,r^2 dr}{\omega_p^2(r)-\omega^2}, \tag{3.52}$$

$$\mathrm{Im}\left\{\mathbf{D}^{BL}(\omega,\mathbf{R})\right\} = e\,\frac{\mathbf{R}}{R^3}\,\frac{\pi}{2}\,\omega^2\,\frac{r_p^2(\omega)}{\left|d\omega_p\left(r_p\right)/dr\right|}\,\theta\left(R-r_p(\omega)\right), \tag{3.53}$$

where $\theta(x)$ is the Heaviside theta function, $V.P.$ is the symbol of the principal integral value.

The total radiating dipole moment of the system IP + atom (ion) is:

$$\mathbf{D}_{tot}(\mathbf{R},\omega) = e_p\,\mathbf{R} - e_p\,\frac{\mathbf{R}}{R^3}\int\limits_0^R \beta\,(r,\omega)\,4\,\pi\,r^2\,dr. \tag{3.54}$$

It should be noted that following from the Eq. 3.54 is the simple relation between the static and polarization dipole moments in the approximation under consideration:

$$\mathbf{D}_{pol}(\mathbf{R},\omega) = \left\{-\frac{1}{R^3}\int\limits_0^R \beta\,(r,\omega)\,4\,\pi\,r^2\,dr\right\}\mathbf{D}_{st}(\mathbf{R},\omega).$$

The formula (3.54) is a primary formula for carrying out numerical calculations of polarization effects in the local approximation. It corresponds to consideration of two channels of the process: static (the first summand in Eq. 3.54) and polarization (the second summand). Since these summands enter into the expression for the total radiating dipole moment of the system target + IP, the expression (3.54), being substituted in the standard formula for the process cross-section or corresponding intensity, will describe also interference effects connected with the interaction of channels.

3.3 Polarization Bremsstrahlung on a Multielectron Ion in the Approximation of Classical Motion of an Incident Particle

As was already noted, the Born parameter η characterizing the motion of plasma electrons under conditions of thermodynamically equilibrium plasma is more or of the order of one:

$$\eta = \frac{Ze^2}{\hbar \mathrm{v}} \geq 1. \tag{3.55}$$

The inequation (3.55) is the reverse of the Born condition and corresponds (in the strong inequality limit) to the quasi-classical approximation for IP motion. It is within the framework of quasi-classics (or, more precisely, of the semiclassical approach) that V.I. Kogans with coworkers [9, 10] have carried out the detailed analysis of the static channel of bremsstrahlung on multielectron atoms and ions. The so-called rotation approximation has been developed that allows rather simple calculation of spectral cross-sections of main radiation processes including photorecombination as well.

The comparison with quantum-mechanical numerical calculations [11] has shown high accuracy of the semiclassical approach and in particular of the rotation approximation in the theory of static Bs.

So it seems natural to use the semiclassical approach also in investigation of polarization Bs on a multielectron ion and to design on its basis the generalization of the rotation approximation including the description of the polarization channel.

As known [12], in classical consideration of a collisional-radiative process the value κ is introduced that is called effective radiation by the formula

$$\kappa = \int_0^\infty \Delta \mathrm{E}(\rho)\, 2\,\pi\,\rho\, d\rho, \tag{3.56}$$

here $\Delta \mathrm{E}(\rho)$ is the total radiation of one IP with the specified impact parameter ρ.

Further we will be interested also in spectral effective radiation $d\kappa(\omega)/d\omega$, the expression for which in the dipole approximation for interaction with an electromagnetic field for a spontaneous process looks like

$$\frac{d\kappa(\omega)}{d\omega} = \frac{4\,\omega^4}{3\,c^3} \int\limits_0^\infty |\mathbf{D}(\omega,\rho)|^2 \rho d\rho, \tag{3.57}$$

where $\mathbf{D}(\omega,\rho)$ is the Fourier transform of the radiating dipole moment of the system at the frequency ω calculated along the trajectory of an IP characterized by the impact parameter ρ.

Between the value $d\kappa/d\omega$ and the spectral cross-section of bremsstrahlung $d\sigma/d\omega$ there is a simple connection:

$$\frac{d\kappa}{d\omega} = \hbar\omega \frac{d\sigma}{d\omega}.$$

To take into account interference-polarization effects, as $\mathbf{D}(\omega,\rho)$, further we will use the temporal Fourier transform of the total dipole moment

$$\mathbf{D}_{tot}(\omega,\rho) = \int\limits_{-\infty}^{+\infty} \mathbf{D}_{tot}(\mathbf{R}(t,\rho,\mathrm{v_i}),\omega) e^{i\omega t} dt, \tag{3.58}$$

in which the function $\mathbf{D}_{tot}(\mathbf{R},\omega)$ is given by the expression (3.54). It should be noted that the dimensionalities of $\mathbf{D}_{tot}(\mathbf{R},\omega)$ and $\mathbf{D}_{tot}(\omega,\rho)$ do not agree: the first value has the dimensionality of the electric dipole moment, and the second value has the dimensionality of its Fourier transform.

Thus in classical calculation of spectral effective radiation it is necessary to know the law of IP motion:

$$\mathbf{R} = \mathbf{R}(t,\rho,\mathrm{v_i}), \tag{3.59}$$

here $\mathrm{v_i}$ is the initial IP velocity.

In investigation of strongly inelastic processes of scattering corresponding to IP motion along strongly curved trajectories it is convenient to express the temporal Fourier transform of the dipole moment of an IP (the first summand of the formula (3.54)) in terms of the Fourier transform of the force acting on the IP on the side of a target. Then from Eq. 3.54 the following expression for the Fourier transform of the total radiating dipole moment of the system (the formula (3.58)) can be obtained:

$$\mathbf{D}_{tot}(\omega,\rho) = \frac{e_p}{m_p\,\omega^2} \left\{ \frac{\mathbf{R}}{R} \frac{dU(R)}{dR} \right\}_{\omega,\rho} - e_p \left\{ \frac{\mathbf{R}}{R^3} \int\limits_0^R \beta(r,\omega)\, 4\,\pi\, r^2 dr \right\}_{\omega,\rho}. \tag{3.60}$$

Here the braces designate taking the Fourier transform in view of the dependence Eq. 3.59.

Thus the expressions (3.56), (3.57), and (3.60) give the formal solution of the problem under consideration. Further simplification of these formulas is impossible since the dependence Eq. 3.59 for IP motion in the Thomas-Fermi potential (and its modifications) has no analytical description (in contrast to motion in the Coulomb field).

To carry out numerical calculations, it is convenient from the independent time variable (t) to go to the independent variable R – the distance from an IP to the nucleus. For this purpose we will use the standard representation of trajectory time and angle of rotation of the IP radius vector in terms of R and the parameters ρ and $\mathrm{v_i}$:

$$t(R,\rho,\mathrm{v_i}) = \int\limits_{r_{\min}(\rho,\mathrm{v_i})}^{\mathrm{R}} \frac{\mathrm{dR}}{\mathrm{v_r}(R,\rho,\mathrm{v_i})} \tag{3.61}$$

$$\varphi(R,\rho,\mathrm{v_i}) = \rho\,\mathrm{v_i} \int\limits_{r_{\min}(\rho,\mathrm{v_i})}^{\mathrm{R}} \frac{\mathrm{dR}}{\mathrm{v_r}(R,\rho,\mathrm{v_i})\,R^2}, \tag{3.62}$$

here $\mathrm{v_r}(R,\rho,\mathrm{v_i})$ is the radial IP velocity, the expression for which looks like

$$\mathrm{v_r}(R,\rho,\mathrm{v_i}) = \sqrt{\mathrm{v_i^2} + 2|U|/m_p - \mathrm{v_i^2}\rho^2/R^2}, \tag{3.63}$$

$r_{\min}(\rho,\mathrm{v_i})$ is the minimum distance of IP approach to the center of the scattering potential determined by solution of the equation

$$\mathrm{v_r}(R,\rho,\mathrm{v_i}) = 0. \tag{3.64}$$

Using the Eqs. 3.60, 3.61, 3.62, and 3.63, it is possible to calculate the Cartesian projections (on the focal axes of coordinates – see Fig. 3.7) of the Fourier transform of the radiating dipole moment of the system according to the formulas:

$$\left(\mathbf{D}_{pol}\right)_x(\omega,\rho) = 2\int\limits_{r_{\min}}^{\infty} \cos(\varphi(R,\rho))\,\cos(\omega\,t(R,\rho))\,D_p(\omega,R)\,\frac{dR}{\mathrm{v_r}(R,\rho)}, \tag{3.65}$$

where $D_p(\omega,R)$ is the magnitude of the vector (3.51).

The expression for $\left(\mathbf{D}_{pol}\right)_y$ is obtained by replacement in Eq. 3.65 of cosines by sines.

The diagram of IP scattering by an atom (ion) with indication of the coordinate axes and the angle φ is presented in Fig. 3.7.

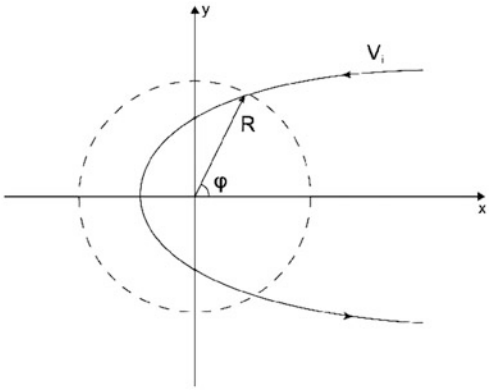

Fig. 3.7 Scattering of an incident particle by a target with the electron core

We will give the results of calculations of spectral effective radiation for electron scattering by a *KII* ion for the following values of parameters $v_i = 1.4$ a.u., $\omega = 0.9$ a.u. The choice of these values is caused by the fact that under conditions of thermodynamically equilibrium plasma of most interest is emission of thermal energy electrons (of the order of the ion ionization potential) of photons with an energy close to the initial IP energy. (The potential of ionization of a *KII* ion is 1.16 a.u.)

To calculate the dipole moment induced in the ion core, we will use the target polarizability density in the Brandt-Lundqvist approximation (the formula (3.35)) shifted in frequency to the value $\Delta\omega = 0.6$ a.u. towards high frequencies. Then the frequency dependence of the dynamic polarizability of the ion core will be approximated to its quantum-mechanical analog.

The electron density of the ion core defining the local plasma frequency was calculated on the basis of numerical integration of the Thomas-Fermi-Dirac equation (with exchange and correlation allowances) with the use of the reduced ionic radius $x_0 = 8.91$ relative units. It will be recalled that the reduced ionic radius is the ratio of the ionic radius R_0 to the Thomas-Fermi radius $a_{TF} = 0.8853/Z^{1/3}$ a.u. In this case the "local plasma radius" (see Eq. 3.38) is $r_p(\omega) = 2.77$ a.u.

Let us introduce into consideration the characteristic radius of radiation in the Kramers limit – $r_{ef}(\omega, v_i)$ – (see [13]), being the solution of the equation

$$\frac{v_i^2}{2} + \frac{|U(r)|}{m_p} = \frac{\omega^2 r^2}{2}. \tag{3.66}$$

This value defines the effective distance of radiation by the static channel. It is essential that in the Kramers limit the value $r_{ef}(\omega, v_i)$ grows with initial velocity.

For the reduced values of parameters and the distribution of electron density of the ion core of a *KII* ion in the Thomas-Fermi-Dirac model we have: $r_{ef}(\omega, v_i) = 1.98$ a.u.

To clarify the appropriateness of using the quasi-classical approach, it should be noted that besides the "global" criterion of quasi-classics (Eq. 3.55), there is also a local criterion that in a three-dimensional case looks like:

$$\eta^{loc}(r) = \frac{\hbar\ \mathrm{div}(\mathbf{p}(\mathbf{r}))}{p^2(\mathbf{r})} << 1. \tag{3.67a}$$

The expression for the local parameter (3.67a) can be rewritten within the framework of the rotation approximation [10] as follows:

$$\eta^{loc}\left(r_{ef}\right) = \hat{\lambda}\left(r_{ef}\right)/r_{ef} << 1, \tag{3.67b}$$

here r_{ef} is given by the formula (3.66). The value (Eq. 3.67b) in the case under consideration is: $\eta^{loc}\left(r_{ef}\right) = 0.22$.

For a special case of a Thomas-Fermi atom (ion) in [10] the analog of the "global" parameter (3.55) was obtained, the reciprocal of which $\varepsilon = 1/\eta$ is given by the formula

$$\varepsilon = \frac{E\, a_{TF}}{Z\, e^2} \equiv 32.6\ \frac{E(\kappa\mathrm{eV})}{Z^{4/3}} \tag{3.67c}$$

Hence for the IP velocity $\mathrm{v_i} = 1.4$ a.u. we find: $\varepsilon = 0.017 << 1$.

Thus the values of the parameters of motion of an IP and a target ion under consideration satisfy the conditions of the quasi-classical approximation for the static Bs spectrum.

The condition of subline quasi-classicity (radiation from the trajectory with a fixed impact parameter ρ) can be written as:

$$\rho\ \mathrm{v_i} \approx \sqrt{l(l+1)} \approx l + 1/2 >> 1. \tag{3.68}$$

The condition (3.68) in our case gives $\rho >> 1$ a.u.

Shown in Fig. 3.8 are the dependences of integrands in the definition of the Fourier transforms of the x- and y-components of the dipole moment induced in the core of a *KII* ion (the real part) on the distance to the nucleus for two values of the impact parameter: (a) $\rho = 1.75$ a.u. and (b) $\rho = 3$ a.u.

In the first case the y-projection of the real part of the induced dipole moment is maximum ($\mathrm{Re}D_y = 2.92$ a.u., $\mathrm{Re}D_x = 1.1$ a.u.), in the second case the x-projection is maximum ($\mathrm{Re}D_x = 2.4$ a.u., $\mathrm{Re}D_y = 1.59$ a.u.).

From Fig. 3.8 it follows in particular that the maximum of the x-component of the dipole moment is reached at the minimum (for the given impact parameter) distance to the ion nucleus. The maximum of the y-component falls on the distance equal to the "plasma" radius $r_p(\omega)$ (for those impact parameters, for which the inequation $r_{\min}(\rho) < r_p(\omega)$ is satisfied).

From Fig. 3.8b it is seen that the integrand for the x-component sharply grows if the equation $r_{\min}(\rho) = r_p(\omega)$ takes place. This equation separates the trajectory of IP motion, at which polarization Bs caused by the x-component of the dipole moment induced in the ion core has maximum.

Let us represent the dependence of the projections of the dipole moments on the impact parameter ρ as a table (Table 3.2).

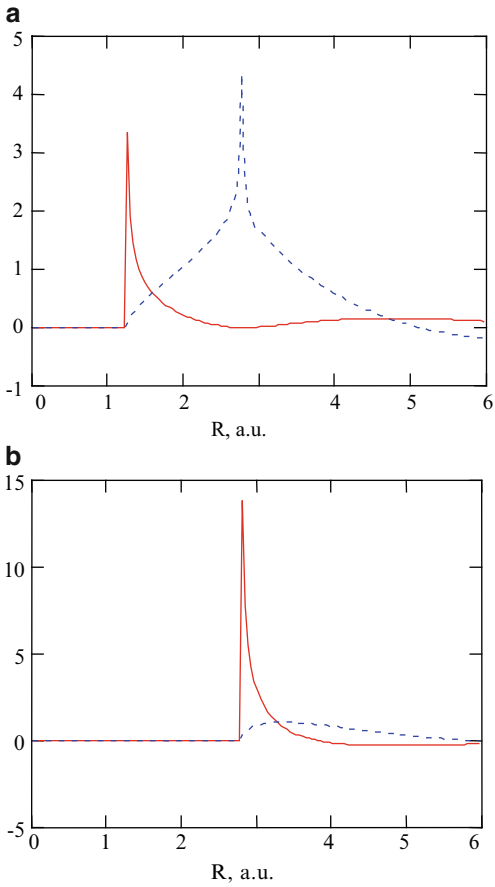

Fig. 3.8 Integrands in the definition of the Fourier transforms of the *x*- (*solid curve*) and *y*- (*dotted curve*) components of the induced dipole moment (the real part) in the core of a *KII* ion ($\omega = 0.9$ a.u., $E = 1$ a.u.) as functions of the distance to the nucleus for the impact parameters: (a) $\rho = 1.75$ a.u. and (**b**) $\rho = 3$ a.u.

Table 3.2 Projections of dipole moments as functions of impact parameter [a.u.]

ρ	1	1.5	2	2.5	3	4	5	6
r_{min}	0.163	0.8	1.58	2.2	2.74	3.76	4.75	5.7
$ReDp_x$	−0.1	1.48	1.0	1.48	2.4	0.73	0.36	0.16
$ReDp_y$	−1.59	2.1	2.9	2.4	1.7	0.86	0.33	0.17
$ImDp_x$	−0.37	1.15	−0.03	−0.22	1.05	0.88	0.29	0.13
$ImDp_y$	−1	0.54	1.1	1.25	1.33	0.68	0.3	0.14

The parameters of calculation were corrected by the conformity of results for the Coulomb potential to exact analytical expressions for the scattering angle.

The calculation in the statistical Thomas-Fermi-Dirac potential shows that for impact parameters lesser than 1.4 a.u. the scattering angle exceeds 180°, which corresponds to beginning of the phenomenon of IP twisting around the target.

On the other hand, for these impact parameters the condition of subline quasi-classical condition is violated, which nevertheless is found to be inessential for

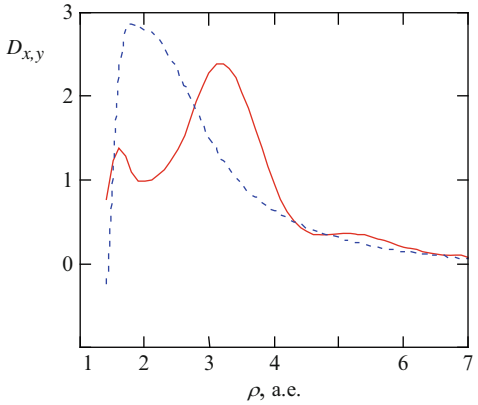

Fig. 3.9 The dependences on the impact parameter of the *x*- (*solid curve*) and *y*- (*dotted curve*) components of the dipole moment induced in the *KII* ion core (the real part) at the frequency $\omega = 0.9$ a.u. in the Brandt-Lundqvist model [5] and the quasi-classical approximation for IP motion

Table 3.3 Effective radiation by the static and polarization channels [a.u.]

Projections, channels	*x*-projection real	imaginary	*y*-projection real	imaginary	Total for each channel
Static	$8.84 \cdot 10^{-6}$		$2.9 \cdot 10^{-6}$		$1.17 \cdot 10^{-5}$
Polarization.	$5.3 \cdot 10^{-6}$	$1.5 \cdot 10^{-6}$	$5.4 \cdot 10^{-6}$	$2.4 \cdot 10^{-6}$	$1.46 \cdot 10^{-5}$

calculation of the polarization channel since small distances to the nucleus make a small contribution to it.

The contribution of these impact parameters ($\rho \leq 1.4$) to effective radiation by the polarization channel is about 1 %.

The obtained dependences of the Fourier transforms $\mathrm{Re}\, D_{x,y}(\omega, \rho)$ on the impact parameter ρ are presented in Fig. 3.9. From this figure it follows in particular that the maximum of the *x*-component of the induced dipole moment in the ion core falls on the impact parameter $\rho_{\max}$ that is approximately equal to the "plasma" radius r_p.

The results of calculation of the values of effective radiation (in atomic units) by the static and polarization bremsstrahlung channels with subdivision to the contributions of the *x*- and *y*-projections are given in Table 3.3.

From Table 3.3 it is seen that in the polarization channel the contribution of the *y*-projection of the dipole moment induced in the core is comparable (and even somewhat exceeds) the contribution of the *x*-projection in contrast to the relation of these contributions to radiation by the static channel. This circumstance is a consequence of the effect of penetration of an IP into the core of a target. This penetration more strongly acts on the *x*-projection, reducing it, than on the *y*-projection. Formally this can be explained by the fact that in motion of an IP along one of the halves of its trajectory its *x*-coordinate changes a sign when crossing the abscissa of the point of

location of the target nucleus, and the y-coordinate is constant-sign and approaches its zero value only at the point of turn of radial IP motion (see Fig. 3.7).

Let us introduce the R-factor characterizing the relative contribution of the polarization channel to bremsstrahlung by the formula:

$$R(\omega) = \frac{d\kappa^{pol}(\omega)}{d\kappa^{st}(\omega)}. \tag{3.69}$$

From the data of Table 3.3 the value of the R-factor in the case under consideration can be determined:

$$\{R\}^{BL}_{clas}(\,\omega = 0.9 \text{ a.u.}, \rho_{\min} = 1.4\,\text{a.u.}) = 1.24. \tag{3.70a}$$

It should be noted that in the value of effective radiation by the static channel an uncertainty remains that is connected with the problem of choosing the lower limit of integration with respect to the impact parameter in the formula (3.36).

For comparative estimation of the relative value of the polarization channel we will use the result of calculation of the static channel contribution within the framework of the rotation approximation (see the paper [10]).

The calculation in the Thomas-Fermi-Dirac model for spectral effective radiation by the static channel gives:

$$\left\{\frac{d\kappa^{rot}_{st}}{d\omega}\right\}_{TFD}(KII,\ \omega = 0.9 \text{ a.u.}) = 5.46 \times 10^{-5}\,\text{a.u.}$$

Hence it follows that the R-factor within the framework of the rotation approximation is:

$$\{R\}^{BL,rot}_{clas,TFD}(KII,\ \omega = 0.9 \text{ a.u.}) = 2.67. \tag{3.70b}$$

However, it should be remembered that the Thomas-Fermi-Dirac model within the framework of the rotation approximation somewhat overestimates the result just for frequencies $\omega \leq 1$ a.u. since in this case the effective radius of radiation r_{ef} (see 3.66) is found to be of the order of the boundary size of an ion, where the statistical model has the greatest error.

So for more correct estimation of effective radiation within the framework of the rotation approximation we use the ion potential in the Slater approximation. Then instead of Eq. 3.70b it can be obtained:

$$\left\{\frac{d\kappa^{rot}_{st}}{d\omega}\right\}_{Slater}(KII,\ \omega = 0.9 \text{ a.u.}) = 4.72 \times 10^{-6}\,\text{a.u.},$$

and correspondingly:

$$\{R\}^{BL,rot}_{clas,Slater}(KII,\ \omega = 0.9 \text{ a.u.}) = 3.1. \tag{3.70c}$$

Thus it can be concluded that the classical estimation for the above values of parameters gives the following lower boundary for the value of the R-factor at a frequency near the potential of ionization of a KII ion for IP of threshold energies (T is the IP energy):

$$R\big(KII,\ \hbar\omega \approx I_p \approx T\big) \geq 2 \tag{3.71}$$

and therefore the contribution of the polarization channel exceeds appreciably the contribution of the static channel to effective radiation of bremsstrahlung.

This conclusion is rather essential since it relates to characteristic "plasma" frequencies (of the order of the ion ionization potential) and a strongly inelastic process, when radiated energy is of the order of the initial IP energy. It is just the situation that is characteristic for Bs in plasma.

3.4 Polarization-Interference Effects in the High-Frequency Limit

From the consideration of effective radiation in collision of an IP with a structural target that was carried out in the previous paragraph within the framework of the classical description of IP motion it follows that the calculation by the obtained formulas is a multistep problem requiring trivariate integration with a singular integrand even for the spectral cross-section. The calculation of the total bremsstrahlung loss, accordingly, results in a quadrivariate integral.

As is known, for static Bs the calculation of total effective radiation is simplified considerably since it is possible to carry out a number of integrations analytically, and the resultant expression (in case of the central potential of scattering) is a single integral, from which all temporal characteristics of IP motion dropped out.

If the polarization channel is taken into account, the situation changes cardinally since the frequency dependence of target polarization in the general case does not allow frequency integration in the expression for total effective polarization radiation.

Assembling the formulas (3.56), (3.57), (3.58), (3.59), and (3.60), we obtain for the total bremsstrahlung loss by the polarization channel in the local plasma frequency approximation:

$$\kappa_{pol} = \frac{4\,e_p^2}{3\,c^3} \int_0^{m_p v_i^2/2\hbar} \omega^4 d\omega \int_0^{\infty} \rho d\rho \left| \int_{-\infty}^{+\infty} dt\, e^{i\omega t} \frac{\mathbf{R}(t,\rho)}{R(t,\rho)^3} \int_0^{R(t,\rho)} \beta(r,\omega)\, 4\pi r^2 dr \right|^2. \tag{3.72}$$

The upper limit of frequency integration reflecting the presence of a short-wavelength limit in Bs is a corollary of quantum relations (the semiclassical approximation [9]) introduced into the classical consideration.

It should be noted that in calculation of the temporal Fourier transform in the formula (3.72) it is possible from time integration to go to integration with respect to the variable distance of an IP to the nucleus R if the radial velocity of IP motion by the formula (3.63) is introduced and the dependences (3.61), (3.62) for the trajectory time and the angle of IP rotation are used.

The description of polarization-interference effects in Bs on a multielectron ion (atom) is simplified considerably in the high-frequency limit, that is, for frequencies much more than the characteristic frequencies of electrons of a target ion. As a result, it appears to be possible to carry out analytical transformations of the formulas describing polarization Bs and to give their descriptive physical interpretation.

Most considerably simplified is the expression for total effective radiation (total bremsstrahlung loss of energy).

Really, in the high-frequency limit the spatial density of the polarizability of the target electron core will be written as:

$$\beta^{hf}(r,\omega) = -\frac{e^2\, n(r)}{m\,\omega^2}. \tag{3.73}$$

It should be noted that the value (3.73) is dimensionless since the concentration of the electron core $n(r)$ has the dimensionality of the reciprocal volume.

For the radiating dipole moment of the core (the polarization channel) with the use of the formulas (3.51) and (3.73) we find the following simple expression:

$$\mathbf{D}^{hf}_{pol}(\mathbf{R},\omega) = e_p \frac{\mathbf{R}}{R^3} \frac{e^2}{m\,\omega^2} N(R), \tag{3.74}$$

here

$$N(R) = \int_0^R n(r)\, 4\,\pi\, r^2\, dr \tag{3.75}$$

is the number of target electrons inside the sphere of the radius R. It should be recalled that R is a distance from an IP to the nucleus of the target.

The physical meaning of Eqs. 3.74 and 3.75 is that the contribution to polarization Bs is made only by the electron density of the target inside the said sphere. The latter is the reflection of the electrostatic fact that a charge placed inside the uniformly charged spherical layer will not experience the Coulomb force. This is true for the process under consideration without real excitation of target electrons since then the core electrons are equivalent to the charge distribution that does not change its geometrical form.

Substituting Eqs. 3.73 in 3.72 results in reduction of frequency degrees, and as a result, changing the order of integration, we obtain:

$$\kappa_{pol}^{hf} = \frac{4\,e_p^2\,e^4}{3\,c^3\,m^2}\int\limits_0^\infty \rho d\rho \int\int dt dt' \int\limits_0^{\mathrm{v}_i^2/2} e^{i\omega(t-t')} d\omega \frac{\mathbf{R}(t)\mathbf{R}(t')}{R^3(t)R^3(t')} N(R(t))N(R(t')). \quad (3.76)$$

Then we use the equation

$$\mathrm{Re}\left\{\int\limits_0^\infty e^{i\omega(t-t')}d\omega\right\} = \pi\delta(t-t').$$

The upper limit here is assumed to be equal to infinity according to the quasi-classical condition $\hbar \to 0$. Going in the formula (3.76) to the integration variable R (after such a replacement the lower limit of integration becomes equal to $r_{\min}(\rho)$, and the result is multiplied by 2 due to the parity of the integrand in the formula (3.76) relative to the change of a time sign) and performing integration with respect to the impact parameter ρ, we find:

$$\kappa_{pol}^{hf} = \frac{8\,\pi\,e^2}{3\,c^3\,m^2\,\mathrm{v}_i}\int\limits_0^\infty f_{pol}^2(r)\sqrt{1-\frac{2U(r)}{m_p\mathrm{v}_i^2}}\,r^2 dr. \quad (3.77)$$

The value $f_{pol}(r)$ appearing here, that is natural to be called polarization force, is determined by the equation:

$$f_{pol}(r) = e_p\,e\frac{N(r)}{r^2}. \quad (3.78)$$

This force (repulsion) acts on an IP on the side of target electrons located inside the sphere of the radius R. With the same force (according to the Newton's third law) the IP accelerates target electrons moving as a single cloud of negative charge, causing polarization Bs.

Let us give here also the expression for total effective radiation by the static channel (see [9]):

$$\kappa_{st} = \frac{8\,\pi\,e_p^2}{3\,c^3\,m_p^2\,\mathrm{v}_i}\int\limits_0^\infty \left(\frac{dU(r)}{dr}\right)^2\sqrt{1-\frac{2\,U(r)}{m_p\mathrm{v}_i^2}}\,r^2 dr. \quad (3.79)$$

It is well seen that the formulas (3.77), (3.79) have a quite similar structure, only the last expression includes the ordinary "static" force:

$$f_{st}(r) = -\frac{dU(r)}{dr}. \quad (3.80)$$

In spite of significant similarity of the Eqs. 3.77 and 3.79, there is also a significant difference between them: the integral of Eq. 3.77 is divergent at the lower limit (in a quasi-classical case as $\int_0 r^{-5/2} dr$) and requires a "cutoff".

The "polarization" integral of Eq. 3.79 at the lower limit is convergent. This is a corollary of taking into account the penetration of an IP into the target core, with the result that the effective electron charge of a ion defining radiation by the polarization channel in the high-frequency limit under consideration decreases.

As a cutoff radius for static effective radiation (3.79), the effective radius of radiation (the formula (3.66)) $r_{ef}(\omega)$ at a frequency corresponding to the initial IP energy is chosen: $\hbar\omega = m\mathrm{v}_i^2/2$.

The formulas (3.76) and (3.77) describe the contribution of each channel to the effective cross-section individually. In fact, in the high-frequency limit under consideration interchannel interference is found to be rather considerable. For total effective radiation of an *electron* the following expression can be obtained in much the same way as this was done above:

$$\kappa_{tot}^{hf} = \frac{8\pi e^2}{3c^3 m^2 \mathrm{v}_i} \int_0^\infty \left(f_{st}(r) - f_{pol}(r)\right)^2 \sqrt{1 - \frac{2U(r)}{m\,\mathrm{v}_i^2}}\, r^2 dr. \tag{3.81}$$

If an effective static charge for an incident electron is introduced by the formula:

$$Z_{ef}(r) = e^{-2} \left| \frac{dU(r)}{dr} \right| r^2, \tag{3.82}$$

then instead of Eq. 3.81 we have:

$$\kappa_{tot}^{hf} = \frac{8\,\pi\, e^6}{3c^3\, m^2\, \mathrm{v}_i} \int_0^\infty \left(N(r) + Z_{ef}(r)\right)^2 \sqrt{1 - \frac{2U(r)}{m\,\mathrm{v}_i^2}}\, r^{-2} dr. \tag{3.83}$$

Hence it is seen that total effective radiation including interchannel interference in the high-frequency limit is defined by the total charge

$$Z = N(r) + Z_{ef}(r) \tag{3.84}$$

that is equal to the charge of the ion nucleus.

To illustrate this fact, given in Fig. 3.10 are the radial dependences of effective polarization (curve 1), static (curve 2), and total (curve 3) charges for a *KII* ion calculated in the Slater model. It is seen that the total charge (3.84) is really equal to the charge of the ion nucleus.

This circumstance is an analog of the effect of atom "stripping" that was for the first time established in the Born approximation [14] for a case of quasi-classical IP motion with penetration into the target core.

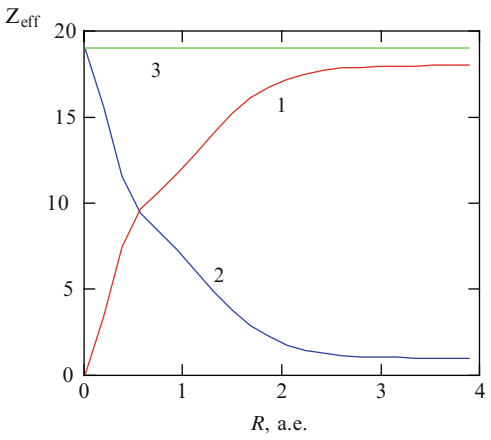

Fig. 3.10 The radial dependences of effective (*1*) polarization, (*2*) static, and (*3*) total charges for a *KII* ion calculated in the Slater model

From Fig. 3.10 it is seen also that the values of effective static and polarization charges are compared for a *KII* ion at a distance about 0.6 a.u. from the nucleus. At longer distances the "polarization" force prevails, at shorter distances the "static" force prevails. In this case it should be remembered that the high-frequency approximation under consideration is true for high enough frequencies

$$\omega > \tilde{\omega}.$$

The analysis shows that the characteristic frequency $\tilde{\omega}$ for a *KII* ion is about 15–20 a.u. (for higher frequencies the polarizability of the target core is close to its high-frequency limit). The effective radii of radiation determined by the Eq. 3.66 in this frequency range satisfy the inequation $r_{ef} < 0.4$ a.u. So the "static" force always exceeds the "polarization" force in the region of truth of the high-frequency approximation.

3.5 Description of Polarization Effects Within the Framework of the Generalized Rotation Approximation

The aim of this paragraph is to simplify the expression for polarization Bs to simple enough calculation formulas. This will allow carrying out numerical estimations of the process cross-sections by the order of magnitude in a wide frequency range in a single manner for any nuclear charges and degrees of target ion ionization and, moreover, it makes it possible to establish qualitative regularities of a phenomenon without resorting to cumbersome calculations. The consistent approach (naturally, within the framework of the plasma model for polarizability) does not allow obtaining simple calculation formulas for *spectral* effective radiation even in the high-frequency limit.

At the same time, as was already said above, in the theory of static Bs there is a rather effective method of approximate calculation of intensity of radiation of a quasi-classical particle, so-called rotation approximation [10], that from the standpoint of the result was found to be more adequate than the consistent classical consideration.

The physical basis of this approach is in the space limitation of a region responsible for radiation by an IP of photons with high enough frequency. The high-frequency behavior, more precisely, the "Kramers behavior", is understood from the standpoint of fulfilment of the inequation [3]:

$$\omega > \omega_{ef}^{Coul} = \frac{m_p \mathrm{v_i}^3}{Z_{ef}\, e_p^2}. \tag{3.85}$$

In this case an IP radiates mainly near the point of turn of its radial motion. It should be noted that quantitatively the rotation approximation also gives a reasonable result in the case $\omega \approx \omega_{ef}^{Coul}$.

For the Bs cross-section integrated with respect to the impact parameter the effective distance (r_{ef}) depends only on the radiated frequency and the target potential and is determined by the Eq. 3.66.

Formally the rotation approximation corresponds to "introduction" into the Eq. 3.60 for total effective static Bs of the delta function of the difference of frequencies ω and the IP rotation frequency at the distance r_{ef}:

$$\omega_{rot}(r) = \frac{\sqrt{\mathrm{v_i}^2 + 2\left|U(r)/m_p\right|}}{r}. \tag{3.86}$$

Thus we come to the following formula for spectral effective radiation *in the rotation approximation* [10]:

$$\left\{\frac{d\kappa_{st}(\omega)}{d\omega}\right\}_{rot} = \frac{8\pi\, e_p^2}{3\, c^3\, m_p^2\, \mathrm{v}_i} \int\limits_0^\infty \left(\frac{dU(r)}{dr}\right)^2 \sqrt{1 - \frac{U(r)}{m_p \mathrm{v}_i^2/2}}\ \delta(\omega - \omega_{rot}(r))\, r^2 dr. \tag{3.87}$$

It seems attractive to generalize the rotation approximation for taking into account radiation by the polarization channel as well.

This is hardly possible to be done strictly since even the static rotation approximation Eq. 3.87 is obtained on the basis of intuitive considerations. So the approach developed below is qualitative, pretending only to the numerical estimation of cross-sections by the order of magnitude.

In the formula (3.87) the information on the vector nature of the radiating dipole moment of an IP is lost. It is connected with the fact that in the high-frequency approximation Eq. 3.85 the main contribution to the process cross-section is made by the x-component of the IP dipole moment. The situation is different for the

polarization channel: for the parameters given in Table 3.3 the contributions of both projections are approximately equal. Therefore in generalization of the rotation approximation for taking into account the polarization channel it is necessary to take into account the features of spatial formation of both Cartesian projections of the dipole moment of the ion core on the axis of the focal system of coordinates.

As seen from Fig. 3.9, the Fourier component of the y-projection of the radiating dipole moment of the target core is defined by the distances of the order of $r_p(\omega)$ (see the formula (3.38)), while the x-component is defined by the distances of most IP approach to the target $r_{\min}$ (the Eq. 3.66).

So it is natural to do the following generalization of the rotation approximation to the polarization channel:

$$\left\{\frac{d\kappa_{pol}(\omega)}{d\omega}\right\}_{rot} = \left\{\frac{d\kappa_{pol}(\omega)}{d\omega}\right\}_{x}^{rot} + \left\{\frac{d\kappa_{pol}(\omega)}{d\omega}\right\}_{y}^{rot}, \tag{3.88}$$

here

$$\left\{\frac{d\kappa_{pol}}{d\omega}\right\}_{x}^{rot} = \frac{8\,\pi\,e^2}{3\,m^2\,c^3\,\mathrm{v_i^2}} \left[\frac{\left|f_x^{pol}(\omega,R)\right|^2 \mathrm{v_r}(R,\rho=0)}{|d\omega_{rot}/dR|}\,R^2\right]_{R=r_{ef}(\omega)} \tag{3.88a}$$

and

$$\left\{\frac{d\kappa_{pol}}{d\omega}\right\}_{y}^{rot} = \frac{8\,\pi\,e^2}{3\,m^2\,c^3\,\mathrm{v_i^2}} \left[\frac{\left|f_y^{pol}(\omega,R)\right|^2 \mathrm{v_r}(R,\rho=0)}{|d\omega_{p}/dR|}\,R^2\right]_{R=r_{p}(\omega)}. \tag{3.88b}$$

The expression for the projection depending on the polarization force frequency is the generalization of the high-frequency analog:

$$f_{x,y}^{pol}(\omega,R) = e_p\,\frac{m\,\omega^2\,R_{x,y}}{e\,R^3}\int_0^R \beta(r,\omega)\;4\pi\,r^2 dr. \tag{3.89}$$

Quantitatively the use of the formula (3.89) instead of Eq. 3.78 means elimination of the abnormally great contribution of low frequencies to the cross-section of polarization Bs arising in case of using the high-frequency approximation near the threshold of target ionization.

It should be noted that the formula (3.89) can be also rewritten in the form similar to Eq. 3.78:

$$f_{x,y}^{pol} = e\,e_p\,\frac{R_{x,y}}{R^3}\;N_{ef}(R,\omega), \tag{3.90}$$

here

$$N_{ef}(R,\omega) = \frac{m\,\omega^2}{e^2}\left|\int_0^R \beta(r,\omega)\,4\,\pi\,r^2\,dr\right| \tag{3.91}$$

is the effective electron charge depending on the frequency and distance to the target nucleus and defining the cross-section of Bs by the polarization channel.

The above formulas for the polarization Bs channel correspond to the simple physical interpretation of this process in the spirit of classical electrodynamics as radiation arising due to acceleration of the effective electron charge of a target under the action of a force from the side of a scattered IP.

According to subdivision of spectral effective radiation by the polarization channel into the sum of contributions of two projections of the induced dipole moment of the target for the spectral R-factor determined by the relation (3.69), within the framework of the generalized rotation approximation it can be written:

$$R^{rot}(\omega) = \frac{1}{2}\left(R_x^{rot}(\omega) + R_y^{rot}(\omega)\right). \tag{3.92}$$

The numerical coefficient in Eq. 3.92 arose due to approximate replacement of the mean squares of sine and cosine of the angle of IP rotation (see Eq. 3.62) by 0.5.

Given in Fig. 3.11a are the frequency dependences of three types of the R-factors appearing in the formula (3.92) for a *KII* ion and threshold energies of an IP. It is essential that the values of the R-factors are compared far from the threshold of target ionization. Near the threshold (for IP energies under consideration) the contribution of the y-component prevails.

The analysis within the framework of the approximation under consideration shows that with growing IP energy the relative contribution of the x-component increases, reaching its maximum value at the energy ($T = m_p\,\mathrm{v}_i^2/2$) determined by the equation:

$$r_{ef}(\omega, T) = r_p(\omega) \tag{3.93}$$

The physical meaning of the formula (3.93) is clear: the generalized rotation approximation predicts the optimum value of initial energy of an IP, at which the effective radius of radiation by the static channel coincides with the "plasma" radius corresponding to the maximum of the spatial density of target polarizability at the given frequency ω. For $\hbar\,\omega = 24.5$ eV the IP energy satisfying the Eq. 3.93 is $T_{opt} = 75$ eV in scattering by a *KII* ion.

Using this model makes it possible to answer an important question: beginning from what frequencies does the high-frequency approximation for the polarization Bs channel work? The comparison of calculation results in the generalized rotation approximation with the high-frequency spectral R-factor is given in Fig. 3.11b.

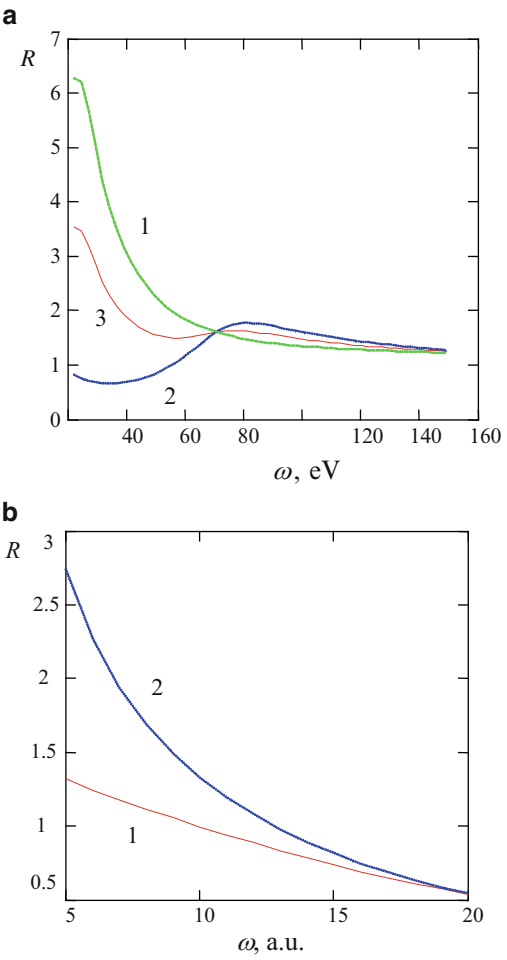

Fig. 3.11 (a) The frequency dependence of the R-factor in different versions of the generalized rotation approximation, when in the PBs cross-section are separated: *1* – "plasma" radius, *2* – effective radius of the static channel, *3* – their half-sum. (**b**) The comparison of the R-factor calculated in the generalized rotation approximation (*1*) with the high-frequency R-factor (*2*) for threshold energies of an IP in its scattering by a *KII* ion

From this figure it is seen that the high-frequency approximation in scattering of an IP of threshold energy by a *KII* ion is true for $\omega > \omega^{rot} = 20$ a.u. With growing IP energy the value ω^{rot} increases.

Let us give the results of calculation of total effective radiation by the polarization channel with the use of the generalized rotation approximation. The corresponding expression (in a somewhat simplified version) looks like:

$$\kappa^{pol}(T) = \frac{8\pi\, e_p^2\, e^4}{3\, c^3 \sqrt{2\, m_p\, T}} \int\limits_{r_{\min}(T)}^{\infty} N_{ef}^2(R,\ \omega_{rot}(R,T)) \sqrt{1 - \frac{U(R)}{T}}\, R^{-2}\, dR, \qquad (3.94)$$

here $r_{\min}(T) = r_{ef}(T,T)$.

Table 3.4 Effective radiation by different channels of a quasi-classical electron on a *KII* ion depending on IP energy

T, a.u. IP energy	3	4	5	10	20
$r_{\min}(T)$, a.u.	1.9	0.95	0.85	0.6	0.42
$\kappa^{st}(T)$ 10^5, a.u. rotation approximation	0.58	0.74	0.86	1.12	1.26
$\kappa^{pol}(T)$ 10^5, a.u. generalized rotation approximation	0.56	0.73	0.86	1.14	1.15
$\kappa^{pol}(T)$ 10^5, a.u. high-frequency approximation	13.2	10	9	5.4	3.2

Though the integral in the formula (3.94) is convergent, we introduced a "cutoff" at the same lower limit as for the static channel since the "non-classical" region of small distances to a nucleus makes a significant contribution for Thomas-Fermi electron distribution overestimating the real electron density near the nucleus. The results of numerical estimations on the basis of the obtained expressions are presented in Table 3.4

In the second line of the table the values of the lower limit in the integrals of Eqs. 3.80 and 3.60 determining total effective radiation by the polarization and static channels are given. It is characteristic for the quasi-classical limit that this value rather weakly decreases with growing IP energy. This defines the weak dependence of total effective radiation on IP energy.

From the calculations carried out within the framework of the generalized rotation approximation it follows that for quasi-classical energies of an incident particle (in terms of fulfilment of the inequations (3.55)) the values of total effective radiation of an electron on a *KII* ion by the static and polarization channels are much the same. The high-frequency approximation overestimates considerably the contribution of the polarization channel, in particular for low IP energies.

The developed approach allows numerical estimations of the contributions of both Bs channels for a wide range of parameters: the charges of ion nuclei Z, the degree of their ionization $q = Z_i/Z$, the frequency of radiation. For this purpose it is convenient to use the Sommerfeld analytical model for the Thomas-Fermi function [7] (see the formulas (A.48) and (A.49)) that makes it possible to carry out calculations rather simply. The results of calculations of the spectral Bs characteristics in the generalized rotation approximation for a wide frequency range and IP of threshold energies ($\hbar\omega \approx T$) are presented in Fig. 3.12a, b.

Following from Fig. 3.12 are the important corollaries of calculations within the framework of the generalized rotation approximation. The contributions of the polarization and static channels to the spectral cross-section of Bs on a *KII* ion for electrons of threshold energies are compared ($R = 1$) at the frequency $\omega^* = 10$ a.u. The maximum of the R-factor is reached for frequencies of the order of the target ionization potential. In this case the generalized rotation approximation gives the following value for the R-factor: $R^{rot}_{\max} \approx 3$. It should be noted that this value represents a lower estimate since the Brandt-Lundqvist model underestimates the value of polarizability.

In the model under consideration the R-factor depends on IP energy (T), growing with T. This has a simple qualitative explanation. With the increase of energy

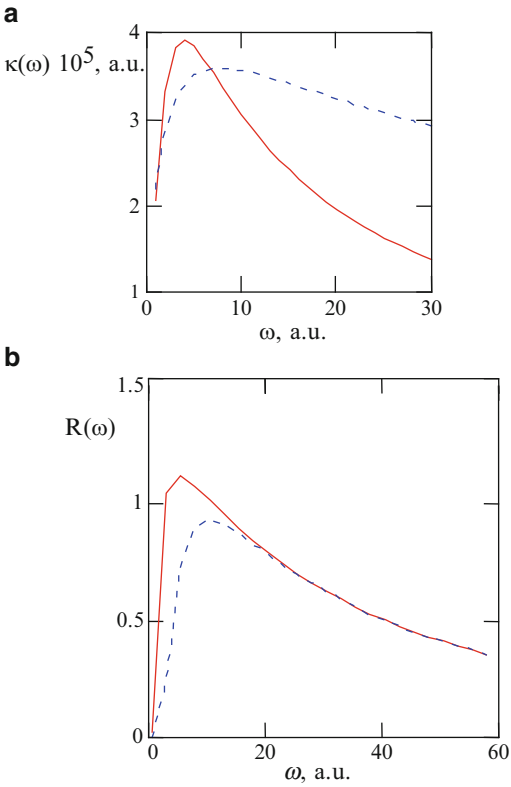

Fig. 3.12 The calculations in the generalized rotation approximation: (a) The spectral dependences of effective radiation of IP of threshold energies by the polarization (*solid curve*) and static (*dotted curve*) channels for $Z = 60$, $q = 0.05$. (**b**) The spectral R-factor for different degrees of ionization: $q = 0.1$ (*solid curve*), $q = 0.2$ (*dotted curve*) and $Z = 60$

(limited by the conditions of usability of the rotation and quasi-classical approximations) the effective radius of the static channel increases: as a result, the effective charge of an ion decreases, the effective electron charge of the core grows.

Given in Fig. 3.12a are the frequency dependences of effective radiation by the polarization (solid curve) and static (dotted curve) channels for a Thomas-Fermi ion (the charge of the nucleus is $Z = 60$, the degree of ionization is $q = 0.05$) up to the kiloelectron-volt energy of a bremsstrahlung photon. It is seen that both dependences have a maximum, and for the polarization channel it is shifted towards lower frequencies. With growing energy of a bremsstrahlung photon effective radiation by the polarization channel (after achievement of the maximum) decreases faster than by the static channel. This is connected with the effect of penetration of an IP into the electron core of a target ion, which, on the one hand, results in increase of the effective charge of the ion defining static Bs, and on the other hand, reduces the dynamic (nondipole) polarizability of the ion core causing polarization Bs.

Presented in Fig. 3.12b are the spectral R-factors for two values of degree of ion ionization: $q = 0.1$ (solid curve), $q = 0.2$ (dotted curve) and the charge of the ion nucleus $Z = 60$. It is seen that the maximum of the R-factor for an ion of lower

charge is reached at lower frequencies, the value of the maximum R-factor is more in magnitude for an ion of a lower degree of ionization. This is explained by higher effective charge and lower nondipole polarizability for an ion of higher charge. With growing photon energy these distinctions (for a multielectron ion) are smoothed, and the values of the R-factors of ions under consideration at higher frequencies are equalized.

Thus it is possible to make a conclusion about the important role of effects of penetration of a radiating electron into the target core for correct description of Bs on multielectron ions of IP of threshold energies. Without considering this phenomenon a qualitatively incorrect result is obtained. For example, the R-factor with growing frequency will tend to the value $1 - q$ (equal to the ratio of the number of bound electrons to the nuclear charge), but not to zero as it should be according to the physics of the process.

Presented in Fig. 3.13a, b are the dependences of the spectral R-factor on the ion charge for different Bs frequencies (a) and nuclear charges (b) calculated for IP of threshold energies. This figure demonstrates the presence (within the framework of the generalized rotation approximation used here) of the optimum ion charge $Z_i^{opt}e$, at which the value of the R-factor (at a frequency characteristic for a given ion) is maximum. This circumstance is a nontrivial fact. Really, for a one-electron ion (and in the case $q \approx 1$) the function $R(Z_i)$ is monotonically decreasing since then the value defining the R-factor is proportional to the reciprocal ion charge: $\omega^2\alpha(\omega)/Z_i(\omega) \propto 1/Z_i$ (for frequencies of the order of the ion ionization potential).

For a multielectron ion the behavior of this dependence is unobvious, and in the general case an answer can be given only within the framework of the approximate description of Bs.

From Fig. 3.13a it follows that the optimum charge $Z_i^{opt}\,e$ grows with decreasing frequency of radiation, and the maximum value of the R-factor in this case somewhat decreases. With growing charge of the ion nucleus (Fig. 3.13b) the value $Z_i^{opt}\,e$ is shifted to the region of high values, and the value of the R-factor appreciably increases. At the same time for low ion charges the R-factors calculated at corresponding (different!) characteristic frequencies do not depend on the nuclear charge.

Let us apply the obtained formulas for calculation of spectral effective radiation in scattering of an electron with an energy of 1 and 10 keV by tungsten ions with different charges. The corresponding diagrams are given in Figs. 3.14 and 3.15. From the given figure it follows that the static channel prevails over the polarization channel throughout the region of frequencies.

With growing IP energy, as seen from Fig. 3.15, a spectral range from 350 to 750 keV takes place, in which the polarization channel prevails over the static channel. According to Figs. 3.14 and 3.15, effective radiation by the polarization channel has a maximum in the low-frequency region of the spectrum that is shifted to the region of high photon energies with increasing IP energy.

Presented in Fig. 3.16 are the calculations of the spectral R-factor (3.69) for Bs of different energies on tungsten ions.

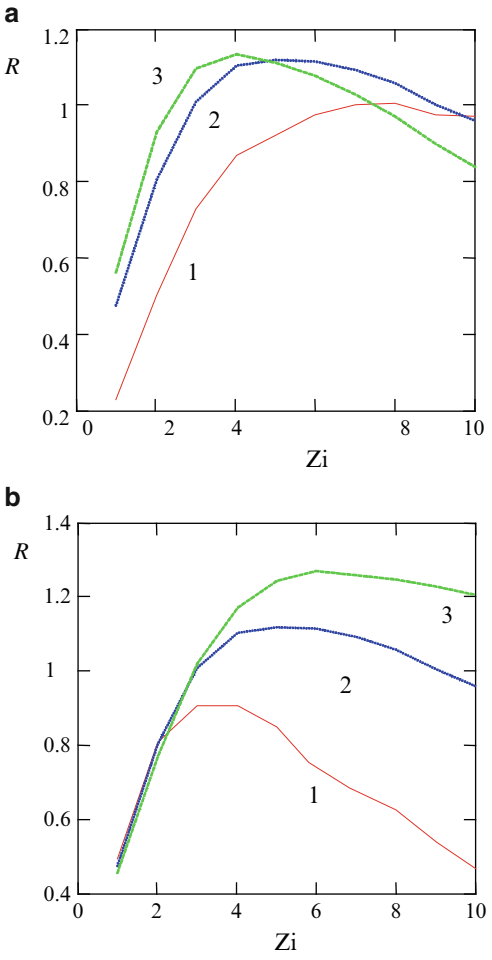

Fig. 3.13 Calculations in the generalized rotation approximation of the dependences of the R-factor on the ion charge at a fixed frequency multiple of the target ionization frequency in the Thomas-Fermi model $\hbar\,\omega = k\,I_p^{TF}$. (a) as functions of the ion charge at different frequencies: $1 - k = 1, 2 - k = 2, 3 - k = 3$. (**b**) the same at the fixed frequency ($\hbar\,\omega = 2\,I_p^{TF}$) for different charges of the ion nucleus: $1 - Z = 30$, $2 - Z = 60$, $3 - Z = 90$

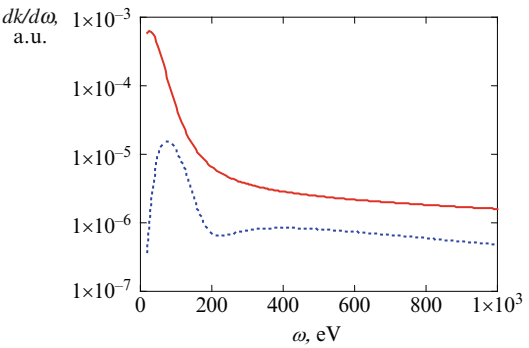

Fig. 3.14 The spectrum of effective radiation in scattering of an electron of energy 1 keV by a tungsten ion with the charge $Z_i = 20$: *solid curve* – static channel, *dotted curve* – polarization channel

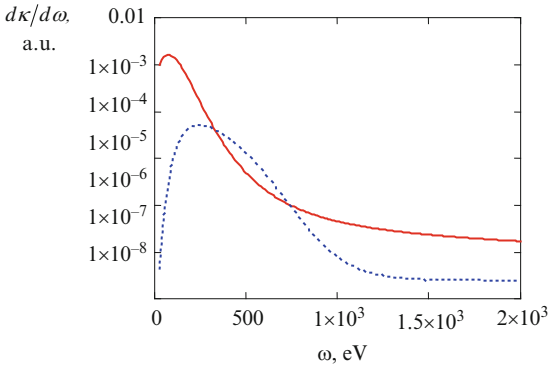

Fig. 3.15 The spectrum of effective radiation in scattering of an electron of energy 10 keV by a tungsten ion with the charge $Z_i = 38$: *solid curve* – static channel, *dotted curve* – polarization channel

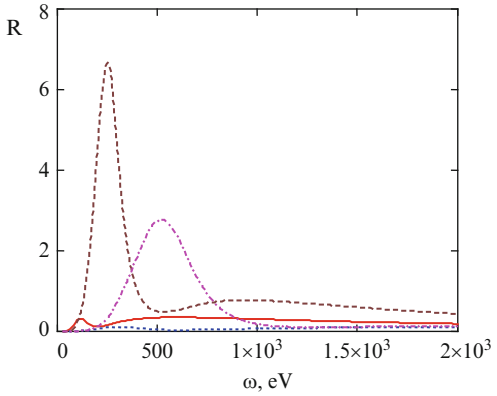

Fig. 3.16 The spectral *R*-factor for Bs on tungsten at different ion charges and IP energies: *solid curve* – Z_i =20, E = 1 keV; *dotted curve* – Z_i =38, E = 1 keV; *dashed curve* – Z_i =20, E = 10 keV; *dash-and-dot curve* – Z_i =38, E =10 keV

It is seen that with growing IP energy (10 keV) the contribution of PBs grows especially for rather low ion charges Z_i =20, when the maximum $R_{max} = 6.8$ is observed in a low-frequency range of the order of 200 keV. With increasing ion charge (at the same IP energy of 10 keV) the maximum of the spectral *R*-factor is shifted to the region of high photon energies (about 500 keV), becoming in this case more wide. In case of low IP energies (1 keV) the *R*-factor is less than one throughout the spectral range for the considered tungsten ions. This is explained by deep penetration of an IP into the ion core for emission of a photon at a low IP energy (1 keV).

Thus the use of the generalized rotation approximation in the description of polarization effects for IP of threshold energies on multielectron ions is found to be rather effective for revealing qualitative regularities of behavior of both Bs channels.

At the end of this paragraph we will make a useful remark on determination of the effective charge of an ion in the rotation approximation $Z_{ef}^{rot}\, e$ (e is the elementary charge) that, in particular, can be used in estimation of effective radiation by the static channel on the basis of the known Kramers formula:

$$\frac{d\kappa^{(Kram)}}{d\omega} = \frac{16\,\pi\, Z_{ef}^2\; e^6}{3\,\sqrt{3}\; m^2\, \mathrm{v}^2\, c^3}\,. \tag{3.95}$$

The matter is that the simple use of the formula (3.79) with substitution of the effective radius of radiation in it leads, generally speaking, to an incorrect result.

The correct expression for the charge number Z_{ef}^{rot} can be obtained from Eq. 3.87 with the use of simple algebraic transformations, it looks like:

$$Z_{ef}^{rot} = \left\{ \frac{r^2\; |dU/dr|}{e\;\sqrt{e^2 + |dU/dr|/(m\,\omega^2 r)}} \right\}_{r=r_{ef}(\omega,T)}, \tag{3.96}$$

where e is the elementary charge.

For Bs on a *KII* ion in the Thomas-Fermi-Dirac model from Eq. 3.96 we find: $Z_{ef}^{rot}(\omega = 0.9\ \text{a.u.},\ T = 1\ \text{a.u.}) = 1.83$ and, accordingly, $d\kappa^{Kr}\big(\omega, Z_{ef}\big)/d\omega = 6.3 \times 10^{-6}$ a.u..

References

1. Landau, L.D., Lifshits, E.M.: The Classical Theory of Fields, 4th edn. Pergamon, New York (1975)
2. Fermi, E.: Uber die Theorie des Stossen zwishen Atomen und electrisch geladenen Teilchen. Z. Physik **29**, 315 (1924)
3. Kogan, V.I., Kukushkin, A.B., Lisitsa, V.S.: Kramers electrodynamics and electron-atomic radiative-collisional processes. Phys. Rep. **213**, 1 (1992)
4. Bethe, H., Heitler, W.: On stopping of fast particles and on creation of positive electrons. Proc. Roy. Soc. Lond. A **146**, 83 (1934)
5. Brandt, W., Lundqvist, S.: Atomic oscillations in the statistical approximation. Phys. Rev. **139**, A612–A617 (1965)
6. Korol', A.V., Lyalin, A.G., Obolenskii, O.I., Solov'yov, A.V.: The role of the polarization mechanism for emission of radiation by atoms over a broad photon frequency range. JETP **87**, 251 (1998)
7. Gombas, P.: Die Statistische Theorie des Atoms und ihre Anwendungen. Springer, Wien (1949)
8. Vinogradov, A.V., Shevelko, V.P.: Static dipole polarizability of atoms and ions in Thomas-Fermi model. Trudy FIAN **119**, 158 (1980) (in Russian)
9. Gervids, V.I., Kogan, V.I.: Penetration and screening effects in electron bremsstrahlung on ions. JETP Lett. **22**, 142 (1975)
10. Kogan, V.I., Kukushkin, A.B.: The emission from quasi-classical electrons in an atomic potential. Sov. Phys. JETP **60**, 665 (1984)

11. Pratt, R.H., Tseng, H.K.: Tip region of the bremsstrahlung spectrum from incident electrons of kinetic energy 50 keV–1.84 MeV. Phys. Rev. A **11**, 1797 (1975)
12. Buimistrov, V.M., Trakhtenberg, L.I.: The role of atomic electrons in bremsstrahlung. Sov. Phys. JETP **46**, 447 (1977)